



Research article

Greenery planning for urban air pollution control based on biomonitoring potential: Explicit emphasis on foliar accumulation of particulate matter (PM) and polycyclic aromatic hydrocarbons (PAHs)



Shritama Mukhopadhyay^{*}, Ratna Dutta^{*}, Papita Das

Department of Chemical Engineering, Jadavpur University, Jadavpur, Kolkata 700032, India

ARTICLE INFO

Keywords:
PM and PAHs
BaP equivalent toxicity
Carcinogenic/mutagenic potential
Leaf micromorphology
Stress responsive leaf traits
APTI/API for green belting

ABSTRACT

In this study, efficiencies of eight indigenous plants of Baishnabghata Patuli Township (BPT), southeast Kolkata, India, were explored as green barrier species and potentials of plant leaves were exploited for biomonitoring of particulate matter (PM) and polycyclic aromatic hydrocarbons (PAHs). The present work focused on studying PM capturing abilities ($539.32\text{--}2766.27 \mu\text{g cm}^{-2}$) of plants (*T. divaricata*, *N. oleander* and *B. acuminata* being the most efficient species in retaining PM) along with the estimation of foliar contents of PM adhered to leaf surfaces (total sPM (large + coarse): $526.59\text{--}2731.76 \mu\text{g cm}^{-2}$) and embedded within waxes (total wPM (large + coarse): $8.73\text{--}34.51 \mu\text{g cm}^{-2}$). SEM imaging used to analyse leaf surfaces affirmed the presence of innate corrugated microstructures as main drivers for particle capture. Accumulation capacities of PAHs of vehicular origin (total index, TI > 4) were compared among the species based on measured concentrations ($159.92\text{--}393.01 \mu\text{g g}^{-1}$) which indicated *T. divaricata*, *P. alba* and *N. cadamba* as highest PAHs accumulators. Specific leaf area (SLA) of plants ($71.01\text{--}376.79 \text{cm}^2 \text{g}^{-1}$), a measure of canopy–atmosphere interface, had great relevance in PAHs diffusion. Relative contribution (>90%) of 4–6 ring PAHs to total carcinogenic equivalent and potential as well as 5–6 ring PAHs to total mutagenic equivalent and potential had also been viewed with respect to benzo[a]pyrene. In-depth analysis of foliar traits and adoption of plant-based ranking strategies (air pollution tolerance index (APTI) and anticipated performance index (API)) provided a rationale for green belting. Each of the naturally selected plant species showed evidences of adaptations during abiotic stress to maximize survival and filtering effects for reductive elimination of ambient PM and PAHs, allowing holistic management of green spaces.

1. Introduction

The severely amplified emission rate of greenhouse gases with other criteria air pollutants results in deterioration of air quality in India which must be tackled on war-footing to ensure sustainable and cleaner environment by avoiding alteration of earth's energy balance and climate. Findings of continuous studies on sustainable practices by the researchers for curbing air pollution have compelled the government bodies of India (like Central Pollution Control Board (CPCB), India) to establish a number of monitoring stations in different states under the National Air Monitoring Programme (NAMP) based on environmental policies and legislative actions (Kaur and Pandey, 2021; NAMP, 2023.). Among the major airborne pollutants, particulate matter (PM) (with size

specification: large (aerodynamic diameter, AD: $10\text{--}100 \mu\text{m}$), coarse (AD: $2.5\text{--}10 \mu\text{m}$) and fine (AD: $\leq 2.5 \mu\text{m}$) and polycyclic aromatic hydrocarbons (PAHs) (including low molecular weight PAHs (LMW PAHs) and high molecular weight PAHs (HMW PAHs)) critically affect human health or any other life form in the ecosphere (Delgado-Saborit et al., 2011; Venkatesan, 2016; WHO, 2006). Overshoot in the anthropogenic emissions, being responsible for a sharp increase in pollutants' generation, has already caused irreversible destruction to the natural environment (Ambade et al., 2022). Remediation efforts must be identified by the scientific society to primarily address the life-threatening challenges posed by the carcinogenic or mutagenic impacts of PAHs and PM with their incidences of prevalence. Health risk evaluation of gaseous and particle-bound PAHs (in terms of benzo[a]pyrene equivalents,

* Corresponding author.

E-mail addresses: mukhopadhyayshritama@gmail.com (S. Mukhopadhyay), paul.ratna@gmail.com, ratna.dutta@jadavpuruniversity.in (R. Dutta), papitasaha@gmail.com (P. Das).

incremental lifetime cancer risks (ILCR) and lifetime average daily dose (LADD)) has indicated that the human exposure increases the lifetime probability of developing cancers in individuals (Morakinyo et al., 2020; Shukla et al., 2022).

Traditional monitoring methods though have provision for discerning location-based real-time air quality trends in relation to actual concentrations of pollutants, they only measure the current concentration of the pollutants in the atmosphere, but never give any idea about long term cumulative accumulation pattern of pollutants. Besides, such methods have limited capacity depending on the suction abilities of the installed air samplers that have to be shifted from one site to other in order to have a greater picture of air quality on a regional basis with spatial gradients. Moreover, they also entail huge expenses for installation and maintenance of facilities at sample locations as well as for manpower deployment for security and continuous maintenance of machineries (Li et al., 2023). From environmental perspective, urban green belts opened out as a fundamental, sustainable and lucrative solution to ambient air pollution control with greater spatio-temporal coverage (Han et al., 2022; Liu et al., 2023; Wu et al., 2021). Multidimensional studies, already carried out with plant leaves, involving theoretical, experimental and computational or simulation approaches, evolved explicit perceptions of phytomonitoring and remediation of PM and PAHs along with the proper understanding of plant-air partitioning (Borgulat and Borgulat, 2023; Pleijel et al., 2022; Redondo-Bermudez et al., 2021; Xie et al., 2022). Therefore, the growing importance of plant foliage in removing and uptaking pollutants has now become apparent relating to their epidermal formations (such as hairy layers, deep grooves, ridges, waxy cuticles, and stomatal abundance), flexible characteristics, macromorphology and larger porous contact surface favourable for adherence, assimilation, internalization and distribution of pollutants in vegetal tissues (De Nicola et al., 2017; Li et al., 2021). Research studies conducted at laboratory scale with optimization trials must also be validated with real-time environmental ambience loaded with manmade interventions replenishing abominably huge quantities of pollutants continuously into the atmosphere (Ghafari et al., 2020). Thus, it is essential to classify the point, non-point and mobile sources of emission for anticipating the nature and characteristics of pollutants contributing to transboundary or local air pollution (Thunis et al., 2019).

The interactions of plants with atmospheric pollutants mediate direct or indirect changes in leaf variables (e.g., chlorophyll, ascorbic acid, sugar, proline, moisture, pH, membrane permeability, wax, trichomes, surface roughness, epidermal cells, stomatal type, etc.) and phenotype which are the expressions of dynamic integrated mechanisms of plant defense against abiotic stress (Anand et al., 2022; Rai, 2016). Since, environmental conditions have profound effects on leaf parameters, analysis of such quantitative traits as biomarkers would yield valuable information on air quality. In relevance with the fact, local plant species growing in overwhelming numbers should have prime weightage for environmental purification through biomonitoring in comparison to the meagrely grown plants (Hajizadeh et al., 2019). In addition to parameter estimation for determining the combinations of plant responsive traits, assessment of species based on air pollution tolerance index (APTI) and anticipated performance index (API) ranking approaches could also assist in green belting configurations in order to improve the filtering effects of tolerant/biomonitor plants (Banerjee et al., 2019; Karmakar and Padhy, 2019). It is worth mentioning that the incorporation of some pollution sensitive plants in green landscaping fulfils the role of indicator species.

Kolkata, one of the Indian megacities, most vulnerable to pollution-induced climatological hazards, has been facing tremendous unplanned growth due to overpopulation for the past few decades, causing unprecedented deterioration of air quality. As a result of which, a number of respiratory airway disorders spiked among 50% of young children (<https://timesofindia.indiatimes.com/city/kolkata/50-of-city-kids-have-air-way-disorder-docs-blame-pollution/articleshow/104956414.cms>) and

over 70% of citizens have been suffering from respiratory illness and reduced life expectancy (by 6.1 years) (<https://timesofindia.indiatimes.com/city/kolkata/breathing-citys-toxic-air-is-like-smoking-doctors/articleshow/63423970.cms>). It is noteworthy that there is a scarcity of studies in Kolkata (specially south Kolkata) exploring biomonitoring perspective for air quality monitoring with emphasis on atmospheric PMs and PAHs concentration and long-term performance of biomonitor to decide upon urban plantations. Research on risk factors of accumulated plant leaf PAHs is also inchoate and needs to be taken up in right earnest. Hence, the current study aimed at (1) estimating the mass fractions of surface-adsorbed and wax-retained PM (large and coarse) deposited on the leaves of eight dominant plant species (trees and shrubs) from the street canyons of Patuli in southeast Kolkata, India, to evaluate their PM retention capacities and quantifying the relationship of leaf waxes, laminar structure and surface micromorphology with particulate capture, (2) measuring the concentrations of foliar PAHs with particular focus on PAHs distribution percentage and profiling based upon ring structure with a view to studying the bioaccumulation pattern for the selected plant species highlighting the significance of specific leaf area (SLA) on total PAHs content, (3) detecting the nature of PAHs (low or high temperature-derived) at the study area through the application of total index, (4) carrying out the toxicity risk analysis of foliar PAHs with reference to the benzo[a]pyrene equivalent concentrations and carcinogenic and mutagenic potential thereof and (5) investigating the feasibility of plant species by examining different plant leaf variables (biomarkers of air quality) with APTI and API screening for urban landscaping.

2. Materials and methods

2.1. Location of sampling site, selection of plant species, sample collection and preservation

In the proposed work, Patuli (Baishnabghata Patuli Township (BPT): 22.4710°N, 88.3924°E) was chosen as the study area which is situated on the southern part of East Kolkata in the state of West Bengal, India. It is well-connected to the Eastern Metropolitan (EM) Bypass (State Highway SH 1) which has very high traffic load and related commercial activities. The BPT site is under the surveillance of a semi-automatic ambient air quality monitoring station (SAAQMS) of West Bengal Pollution Control Board (WBPCB), which has prompted us to select the sampling points (near Benubana Chhaya: water park and garden, Patuli overbridge and Metropolis shopping mall) within such area due to the possibility of high load of urban pollution. The location of the study area along with a route map has been depicted in Fig. 1a and b highlighting the sampling spots which are adjacent to and surrounded by SH 1 (EM Bypass), super specialty hospitals, modern housing complexes, many big commercial outlets and metro train line. Moreover, air quality data given by WBPCB for three criteria pollutants, PM₁₀, SO₂ and NO₂, across the site throughout the sampling time have been presented in Table 1 to recognize the aggravated air quality of the selected sites in Kolkata metro city.

The most common roadside plants of varied life forms (shrubs and trees), nature (evergreen and deciduous) and leaf types, such as *Nerium oleander* (Local name: Rakta Karabi, Family: Apocynaceae), *Tabernaemontana divaricata* (Local name: Tagar, Family: Apocynaceae), *Catotropis gigantea* (Local name: Akanda, Family: Apocynaceae), *Bauhinia acuminata* (Local name: Kanchan, Family: Fabaceae), *Polyalthia longifolia* (Local name: Debdaru, Family: Annonaceae), *Alstonia scholaris* (Local name: Chhatim, Family: Apocynaceae), *Neolamarckia cadamba* (Local name: Kadam, Family: Rubiaceae) and *Plumeria alba* (Local name: Champa, Family: Apocynaceae) were selected to examine the potential to act as vegetation barriers (with diversifying plant communities) for mitigation of air pollution. Hence, in accordance with the current study, fully expanded and matured leaves were sampled using stainless steel garden scissors with proper precaution, in the peak hours at morning,

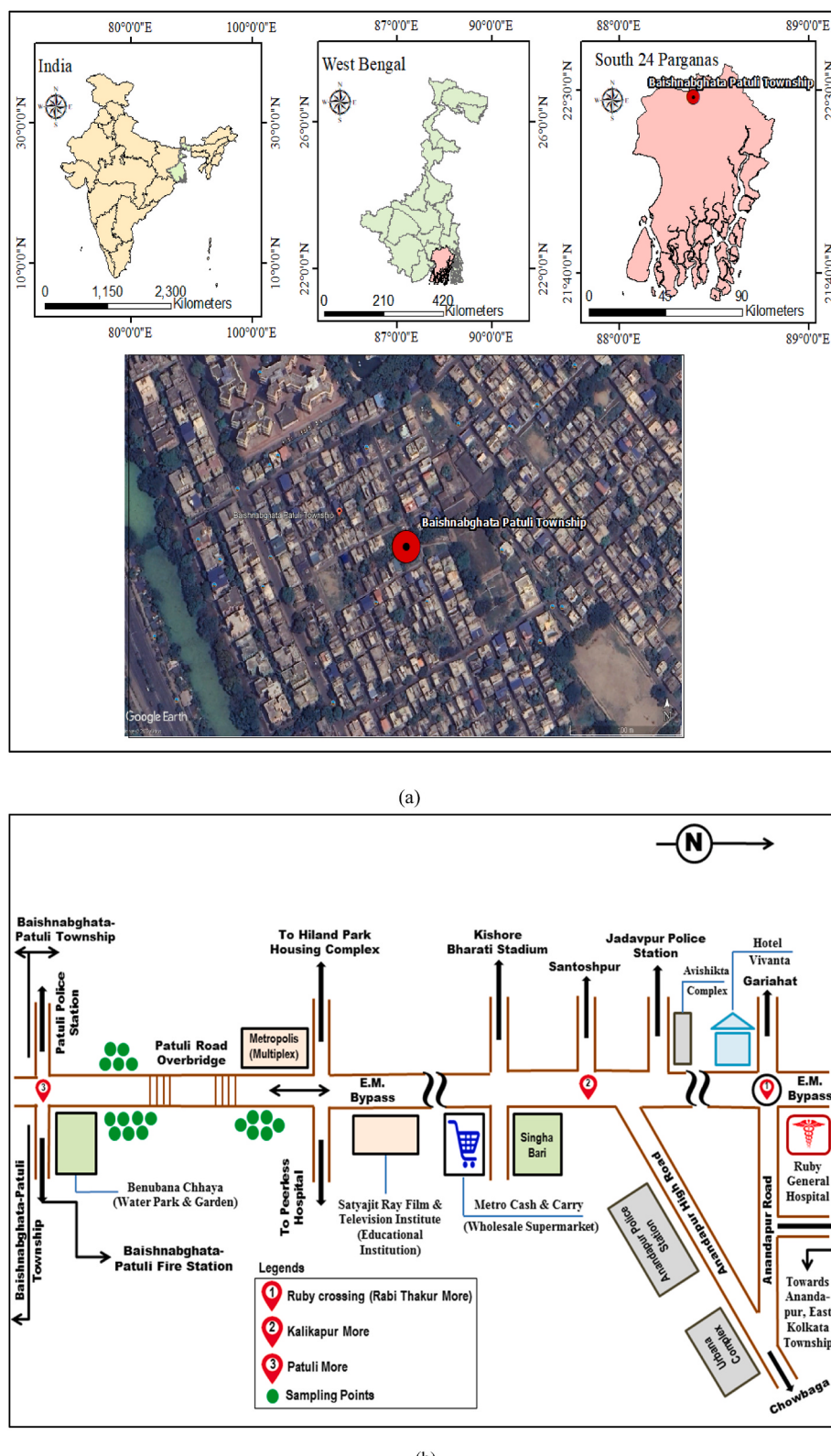


Fig. 1. (a) Location of the study area (Baishnabghata Patuli Township, BPT) within Kolkata, West Bengal, India and (b) route map view of sampling at Patuli.

from the road-facing branches of different individual plants of same species as available within 3 m height from ground level in the selected spots during January–March 2021. The collected samples (including the replicates of each species) were then kept in polyethylene sample bags and directly taken to the laboratory for further investigation (Yang et al.,

2017). The plant leaves were processed to fine powder in a mortar after rinsing with deionized water (for the removal of extraneous materials (biological or non-biological) from foliar surfaces) and lyophilization and ultimately stored for leaf tissue analysis (De Nicola et al., 2016; Foan and Simon, 2012). Fresh leaves were also utilized for some parametric

Table 1

Air quality information of BPT area based on the data of WBPCB monitoring station during the sampling period (http://emis.wbpcb.gov.in/airquality/filter_for_aqi.jsp).

Month	Sampling date	Ambient air quality monitoring data				Air quality status
		NO ₂ (µg m ⁻³)	SO ₂ (µg m ⁻³)	PM ₁₀ (µg m ⁻³)	Air quality index with respect to PM ₁₀ (Range)	
	Permissible limit (24 h average)	80	80	100		
January	January 15, 2021	49	9	226	184 (101–200)	Moderate
	January 18, 2021	49	9	274	224 (201–300)	Poor
	January 24, 2021	48	10	276	226 (201–300)	Poor
February	February 02, 2021	52	10	267	217 (201–300)	Poor
	February 11, 2021	45	9	172	148 (101–200)	Moderate
	February 17, 2021	51	9	239	193 (101–200)	Moderate
March	March 03, 2021	51	9	188	159 (101–200)	Moderate
	March 13, 2021	47	9	205	170 (101–200)	Moderate
	March 19, 2021	52	10	244	196 (101–200)	Moderate

tests, like measurements of PM, RWC, membrane stability index and electrolyte leakage as well as for morphological examination.

2.2. Quantitative estimation of particulate matter (PM) retained on plant foliage and leaf waxes

Assessment of the contents of PM deposited on plant leaves (surface PM or sPM) and that entrapped in leaf waxes (wax PM or wPM) was accomplished in accordance with the method elaborated by Dzierznowski et al. (2011). Leaf samples were kept in Erlenmeyer flasks and thoroughly washed with 250 mL of deionized water aided by agitation for 1 min to wash out the surface-adsorbed particulates. For eliminating particles of size >100 µm, the washed-out solutions were first filtered through a metal sieve. Sequential filtration was also carried out afterwards using pre-weighed Whatman Grade 1 filter paper to collect large fraction of PM (ranging between 10 and 100 µm) and Whatman Grade 42 filter paper for the retention of coarse PM (2.5–10 µm) by the help of a filtration unit with porcelain Buchner funnel fitted to a portable oil-free vacuum pump (Rivotek). Filters were again oven-dried post-filtration at 60–70 °C for about 30 min and mass of each PM fraction was noted.

The plant leaves, already washed with water, were immersed in 150 mL of chloroform and shaken for 40 s to extract the wax-embedded PM for its quantification through the same filtration procedure as stated above. Total PM load was defined as the summation of sPM and wPM (i.e. summation of total large PM = large (sPM + wPM) and total coarse PM = coarse (sPM + wPM)). The resulting extracts containing dissolved waxes in chloroform were transferred to different pre-weighed vials, dried for solvent evaporation and thereafter accurately weighed as leaf waxes. Total areas of all the leaf samples were calculated using graph papers (Prajapati and Tripathi, 2008a), which were then utilized to express the content of PM deposited and waxes in µg cm⁻² of leaf area. Specific leaf areas (SLAs) were also evaluated with the estimated values of leaf area (A, cm²) and leaf dry weight (DW, g):

$$SLA \left(\text{cm}^2 \text{g}^{-1} \right) = \frac{A}{DW} \quad (1)$$

2.3. Analysis of leaf core attributes to discern the biomonitoring potential of the selected plant species

2.3.1. Total chlorophyll, carotenoid and ascorbic acid contents

Leaf chlorophyll (Chl) and carotenoid concentrations were determined by classical spectrophotometric method, wherein, 1 g sample was extracted with 20 mL of acetone:water mixture (80:20, v/v) under stirring for 15 min at ambient temperature followed by extract filtration

and refrigerated storage (Sudhakar et al., 2016). The extraction was repeated five times until complete removal of pigments from the leaf matrix was anticipated.

Plant leaves were analysed for ascorbic acid (AA) content using the standard 2,6-dichlorophenol indophenol (DCPIP, AR/ACS grade, assay: 98%; Loba Chemie, India) titration method (Roy et al., 2020).

The measurement protocols along with the formulae for estimation of chlorophyll, carotenoid and ascorbic acid contents have been elaborated in the 'Supplementary section'.

2.3.2. Relative water content and foliar pH

Appropriate measurement of relative water content (RWC) of sampled leaf tissues was performed considering leaf fresh weight, turgid weight (acquired after water saturation of the leaves kept overnight in submerged condition) and dry weight (obtained after drying of leaves in hot air oven at 70–80 °C) (Pathak et al., 2011) (for further details, refer 'Supplementary section').

pH of the filtered leaf extracts was monitored using a LT-23 digital pH meter (Labtronics, India) calibrated with standard buffer capsules of pH 4 and 9, after homogenization of 2 g of sample in 40 mL of double distilled water (Zhang et al., 2016).

2.3.3. Membrane stability index and electrolyte leakage

Fresh plant leaves of each species were cut into small circular discs which were then immersed in 20 mL of deionized water-filled glass beakers and incubated for 2–3 h at room temperature. Initial electrical conductivity (EC₁) of the solution was measured with a benchtop digital conductivity meter (Labtronics, Model: LT-23). The glass beakers were placed in boiling water bath for 15 min and again cooled down to room temperature in order to record the final electrical conductivity values (EC₂). The membrane stability index (MSI in %) and electrolyte leakage (EL in %) were evaluated in terms of conductance due to ion leakage from the foliar tissues applying the below-mentioned formulae (Mukherjee et al., 2020; Singh et al., 2007):

$$MSI (\%) = \left(EC_2 - \frac{EC_1}{EC_2} \right) \times 100 \quad (2)$$

$$EL (\%) = \left(\frac{EC_1}{EC_2} \right) \times 100 \quad (3)$$

2.3.4. Leaf carbon content

Carbon content of plant leaves was quantitated by loss on ignition method which is a simple, rapid and cost-effective technique widely employed for larger sample sizes (Paull et al., 2021). Initially, the leaves were oven-dried at 70–80 °C for 48 h and consequently, 1 g of dried

sample was subjected to the process of dry ashing at 550 °C temperature for 3 h using a muffle furnace (Baxter et al., 2014). Content of leaf carbon was then obtained as:

$$LOI = \frac{DW - AW}{DW} \times 100 \quad (4)$$

where, LOI = loss on ignition (%), DW = dry weight of sample (g) and AW = ash weight of sample (g).

2.3.5. Protein, proline and total soluble sugar contents

Quantification of proteins in plant leaves was carried out using a colorimetric assay, i.e., Bradford method (Bradford, 1976). Primarily, leaf protein extracts were obtained after grinding of dried foliar tissues (2 g for each extraction) in 5–10 mL of extraction buffer (STET lysis buffer; SRL, India) with mortar pestle accompanied by centrifugation. For analysing the protein content of all the leaf samples, 5 mL of Bradford reagent (SRL, India) was added to 0.1 mL of each extract in separate test tubes, mixed thoroughly and incubated for 5–10 min. Absorbances of the solutions were then recorded at 595 nm by a UV/Vis spectrophotometer (PerkinElmer, USA; L365) with reference to a reagent blank (composed of 0.1 mL extraction buffer and 5 mL Bradford reagent). Protein concentrations were thus determined against a calibration curve of commercial bovine serum albumin (BSA, assay: 98%; SRL, India) prepared by a series of standards diluted from the BSA stock of 2 mg mL⁻¹ in extraction buffer and computed on a dry weight basis in mg g⁻¹.

Proline content of plant leaves was assessed according to the protocol proposed by Bates et al. (1973) using ninhydrin reagent. Leaf tissues (1 g) were first macerated in an aqueous solution (3% w/v) of sulfosalicylic acid (extrapure, 99%; SRL, India) (20 mL). After homogenization, tissue homogenates were centrifuged at 2800 rpm for 10 min. The supernatants were collected thereafter in glass vials for analysis, wherein, 2 mL of ninhydrin reagent (extrapure AR/ACS grade, 99%; SRL, India) (prepared by dissolving 1.25 g in a solution of glacial acetic acid (ACS reagent, ≥99.7%; Merck, Darmstadt, Germany) (30 mL), deionized water (15 mL) and 85% ortho-phosphoric acid (extrapure, assay: 85%; SRL, India) (5 mL) (6:3:1) (Ncube et al., 2013)) and 2 mL of glacial acetic acid were added to different test tubes containing 2 mL of extract. The sample tubes with mixture were kept in boiling water bath for 1 h and 4 mL of toluene was then added to each tube after cooling them down to room temperature. Upon vigorous mixing, the organic (toluene or chromophore) layer was pipetted out and transferred to glass cuvettes for absorbance reading at 520 nm as against a sample blank with only toluene. A standard curve (of pure proline (99% by assay; SRL, India) with initial stock of 0.1 mg mL⁻¹) was used for calculating the unknown concentrations of proline in the test samples in mg g⁻¹ DW of leaves.

To isolate and quantify total soluble sugars, ground foliar tissues (1.5 g) were subjected to sequential extractions (three times for 5 min each) using 15 mL of hot ethanol (80%). The clear extracts were recovered after centrifugation and 2 mL aliquot of the extracts transferred in each test tube was mixed with 5 mL of 5% (w/v) zinc sulphate (pure, 99%; SRL, India) and 4.7 mL of 0.3 (N) barium hydroxide (pure, 98%; SRL, India) solutions. The mixtures were vigorously shaken and again centrifuged for 10 min at 2800 rpm. 4 mL of anthrone reagent (extrapure AR, 98%; SRL, India) solution (of standard composition — 2 g dissolved in 1 L of concentrated sulphuric acid) was then added to 0.5 mL aliquot of the collected supernatant in glass tubes and heated to 90–100 °C for 10 min. The resulting solutions were allowed to cool down and consequently analysed spectrophotometrically at 630 nm in respect of a blank (1 mL distilled water and 5 mL reagent) (Sarabi and Arjmand-Ghajur, 2021). Quantitation of total soluble sugars was performed based on a standard curve of varying concentrations of glucose (extrapure AR/ACS; SRL, India) made from the stock of 0.2 mg mL⁻¹ and expressed in mg g⁻¹ DW of leaves.

2.4. Air pollution tolerance index (APTI)

Plants' inherent ability to combat air pollution was examined through the estimation of APTI based on the formula (Singh et al., 1991) involving biochemical and physiological markers, such as Chl, AA, RWC and pH, as indicated below:

$$APTI = \frac{A \times (T + P) + R}{10} \quad (5)$$

where, where, A = ascorbic acid content (mg g⁻¹), T = total chlorophyll content (mg g⁻¹), P = leaf extract pH and R = relative water content (%).

2.5. Anticipated performance index (API)

Feasibility of plant species for green belting to help in ecological restoration was assessed by API which particularly depends on several biological, biochemical and socioeconomic characteristics of plants including APTI, type of plant and growth habit, arrangement of plant canopy, laminar structure and economic value (Pandey et al., 2015a, 2015b; Prajapati and Tripathi, 2008b). API is based on a grading system where each plant is assigned with a grade (+)/(-) owing to its traits, totalling up to 16 positive points and leading to a percentage evaluation (% score) as given by the following formula:

$$\% \text{ Score} = \frac{\text{Total grades obtained by the plant species}}{\text{Maximum possible grades for any plant species (16)}} \times 100 \quad (6)$$

API values were determined for all the plants corresponding to their respective % score, to finally ensure their category for utilization in urban landscaping.

2.6. Investigation of leaf surface micromorphology

The adaxial and abaxial surfaces of plant leaves were studied with the help of a scanning electron microscope (SEM, Hitachi S-3400 N) for minute observations of leaf surface microstructures and epidermal characteristics along with PM deposition. The SEM images (with magnification range of 35X–3000X) were finally acquired under high vacuum at an accelerating voltage of 15 kV. The overall procedure of sample preparation is provided in the 'Supplementary section'.

2.7. PAHs determination in plant foliage

Prior to analysis, the process of Soxhlet extraction was employed, where 120 mL of toluene was used to extract PAHs from plant leaves (10 g for each sample) for 6 h and the specific fractions of PAHs were separated using silica gel (high purity grade, 100–200 mesh; Merck, Darmstadt, Germany) column as previously reported in Mukhopadhyay et al. (2023). The collected fractions were almost concentrated to dryness via rotary evaporation (Rotavapor R-3, Buchi) and solvent-exchanged to analytical grade methanol for high performance liquid chromatographic (HPLC) analysis. Details of the analytical protocol have been given in the 'Supplementary section'.

2.8. Risk factor assessment

Risks associated to PAHs were evaluated by means of carcinogenic and mutagenic equivalent concentrations (BaP_{TEQ} and BaP_{MEQ} in µg g⁻¹ respectively) relative to BaP (which is regarded as an indicator of carcinogenic PAHs). Individual toxicity (i.e. carcinogenicity and mutagenicity) of each PAH congener was calculated by multiplying the measured foliar concentration of every PAH compound (PAH_i) with its toxic equivalency factor (TEF) (Nisbet and LaGoy, 1992) and mutagenic equivalency factor (MEF) (Durant et al., 1996). Values of BaP_{TEQ} (for all the 16 PAHs) and BaP_{MEQ} (for BaA, CHR, BbF, BkF, BaP, DB[ah]A, IP and B[ghi]P) were then summed up to estimate the total carcinogenic

and mutagenic potencies of PAHs present in the matrix (denoted in Eq. (7) and Eq. (8)) (Ihunwo et al., 2021; Verma et al., 2022) with the assumption that the toxicity of all the individual PAHs would be additive (USEPA, 2002; WHO, 2000). Contribution of each PAH to total risk potency was also determined in terms of carcinogenic and mutagenic potential (CP and MP in %) as represented below in Eq. (9) and Eq. (10) (Blaszczyk et al., 2017; Delgado-Saborit et al., 2011):

$$BaP_{TEQ} = \sum_{i=1}^N PAH_i \times TEF_i \quad (7)$$

$$BaP_{MEQ} = \sum_{i=1}^N PAH_i \times MEF_i \quad (8)$$

$$CP_i = \frac{\frac{PAH_i}{BaP} \times TEF_i}{\sum_{i=1}^N \frac{PAH_i}{BaP} \times TEF_i} \times 100 \quad (9)$$

$$MP_i = \frac{\frac{PAH_i}{BaP} \times MEF_i}{\sum_{i=1}^N \frac{PAH_i}{BaP} \times MEF_i} \times 100 \quad (10)$$

2.9. Statistical analysis

The results have been reported in terms of standard deviation (SD) as mean \pm SD of each dataset of triplicate values. Statistical analysis was carried out using one-way and two-way ANOVA in Microsoft Excel in order to express the significance of the data variability. Correlation coefficient (r) was estimated to reveal the positive or negative linear relationships between PM and PAHs and between PM or PAHs with each of the different leaf variables (biochemical, physiological and morphological). The same was also performed between some of the leaf traits to understand their strength of relationship. The significance threshold was maintained at $p < 0.05$ for data acceptability and reliability.

3. Results and discussion

3.1. PM capturing potential of plant leaves: impacts of environmental influence, leaf waxes and morphology

The competence of plants for particulate retention plays a pivotal role in selection of species for designing of urban green spaces, leading to sustained source of environmental comfort and protection. PM reduction by plants from the ambient air involves discrete mitigative mechanisms — diffusion, impaction, interception, sedimentation and a combination thereof and is governed by the abundance, diversity and arrangement of plant species in a vegetation cover (taking into account leaf traits, phenology, tree measurement, crown spread and plant growth characteristics), actual distance of the green zone from the original source of emissions as well as particle sizes and concentration (Brantley et al., 2014; Huang et al., 2013; Janhall, 2015). Foliar micromorphology, properties of leaf cuticle and environmental factors including weather and climate change, landscape ecology and human settlements also have considerable impacts on deposition and accumulation of PM on plant leaves (Thompson, 2018).

The mass of different size fractions of PM captured by the surfaces and cuticular waxes of plant leaves has been demonstrated in Fig. 2a and b. The occurrence of high concentrations of PM in the study area is directly related to the level of pollution from atmospheric stability (most common in winter months) and anthropogenic factors, such as construction activities, heterogeneous fleet of vehicles, high traffic flow and volume, turbulences generated by motor vehicles, urban road/street design and existence of various types of roadside buildings/business establishments. Significant variability ($F > F_{crit}$ and $p < 0.05$) between the accumulation of both sPM and wPM were noticed among all the

species applying one-way ANOVA along with significant differences in their total loads. It was found that the large particles (10–100 μm) were dominant ($493 \pm 91.70 - 2680 \pm 78.85 \mu\text{g cm}^{-2}$) in the deposition of PM on leaf surfaces as compared to the coarse PM (2.5–10 μm) ($33.59 \pm 13.68 - 86.51 \pm 19.45 \mu\text{g cm}^{-2}$) (ref. Fig. 2a) and the total sPM (large + coarse) load on the plant foliages ranged between $526.59 \pm 105.38 - 2731.76 \pm 96.39 \mu\text{g cm}^{-2}$. In cuticular/epicuticular waxes, though different PM fractions were trapped, total accumulation of large and coarse particulates (total wPM: $8.73 \pm 1.39 - 34.51 \pm 9.61 \mu\text{g cm}^{-2}$) was observed to be less with respect to surface deposition (ref. Fig. 2b). Also, individual concentrations of large ($5.30 \pm 1.19 - 25.82 \pm 7.54 \mu\text{g cm}^{-2}$) and coarse ($1.77 \pm 0.62 - 15.34 \pm 5.48 \mu\text{g cm}^{-2}$) PM in wax layers were much less than those of the surfaces in all the plant species examined. The probable reason could be that the immobilisation of PM in waxes is not prompt but a time-intensive process, less dependent on weather variations, unlike sPM which is strongly influenced by the impact of weather turbulences (Lu et al., 2019). For spruce, black pine and juniper species, Xu et al. (2019) reported 1.58–3.33 times higher PM retention by leaf surfaces than that of waxy layers. Przybysz et al. (2019) and Zhou et al. (2022) also obtained comparable results in case of tree species (*T. baccata* L., *P. nigra* L. and *C. betulus* L.) and evergreen shrubs (*R. pulchrum*, *O. fragrans* and *P. fraseri*) respectively. Predominantly, highest proportion of large-sized PM was recorded for all the eight species, while leaf retention accounted for lowest proportion of coarse particles. This might be due to the fact that larger particles have high propensity to settle at a faster rate under gravity, thereby facilitating foliar retention, in comparison to the coarse PM which is most likely to be transported by air before their deposition on environmental surfaces (Lu et al., 2019). Dzierzanowski et al. (2011), Konczak et al. (2021) and Przybysz et al. (2019) studied PM accumulation with plant species diversity (leafy trees, conifers, shrubs, climbers and vines) and noticed maximum contribution of large-sized particulates to the total mass of accumulated PM.

The PM retention capacity ($\mu\text{g cm}^{-2}$) of the plants varied in the order of: *Tabernaemontana divaricata* (2766.27 ± 86.79) > *Nerium oleander* (1808.64 ± 46.99) > *Bauhinia acuminata* (1697.57 ± 95.76) > *Polyalthia longifolia* (1100.44 ± 94.77) > *Plumeria alba* (1054.27 ± 112.85) > *Alstonia scholaris* (932.61 ± 89.93) > *Calotropis gigantea* (709.91 ± 71.34) > *Neolamarckia cadamba* (539.32 ± 101.49). Many studies have reported pronounced contribution of leaf waxes on PM accumulation (Popek et al., 2015, 2022; Przybysz et al., 2019; Saebo et al., 2012). In the present study, quantity of waxes ranged between $23.69 \pm 3.83 - 182.12 \pm 24.95 \mu\text{g cm}^{-2}$ in all the species (ref. Fig. 2c). It was observed that *T. divaricata* showing highest accumulation of total PM displayed maximum wax content, followed by *N. oleander*. On the other hand, *C. gigantea* and *N. cadamba* presented minimum wax contents with least PM capturing capacities. The other four species (namely, *B. acuminata*, *P. longifolia*, *P. alba* and *A. scholaris*) did not follow the similar trend. Hence, it could be inferred from above that the PM accumulation would depend not only on the foliage concentrations of waxes, but also on the chemical constituents and structure of the wax layers which determine the area of interfacial surface in addition to adhesion, uptake and translocation of particles (Corada et al., 2021; Lukowski et al., 2020; Popek et al., 2015; Saebo et al., 2012). Considering all the species together, positive correlations were obtained between wax content and total large PM ($r = 0.89$, $p < 0.05$), total coarse PM ($r = 0.45$, $p > 0.05$), total PM ($r = 0.89$, $p < 0.05$), total sPM ($r = 0.89$, $p < 0.05$) and total wPM ($r = 0.68$, $p < 0.05$) loads. However, it can be seen from the above results that the variation between wax content and total coarse PM is not very much significant. The current findings are in line with the previous researches, conducted by Lukowski et al. (2020) and Popek et al. (2022), where leaf wax contents were positively correlated to the PM load.

The shape of the plant leaves also significantly controls PM accumulation (Saebo et al., 2012; Weerakkody et al., 2018). Interaction of plant leaves having different shapes, texture and flexible porous structures with the wind generate variable drag forces on the foliages,

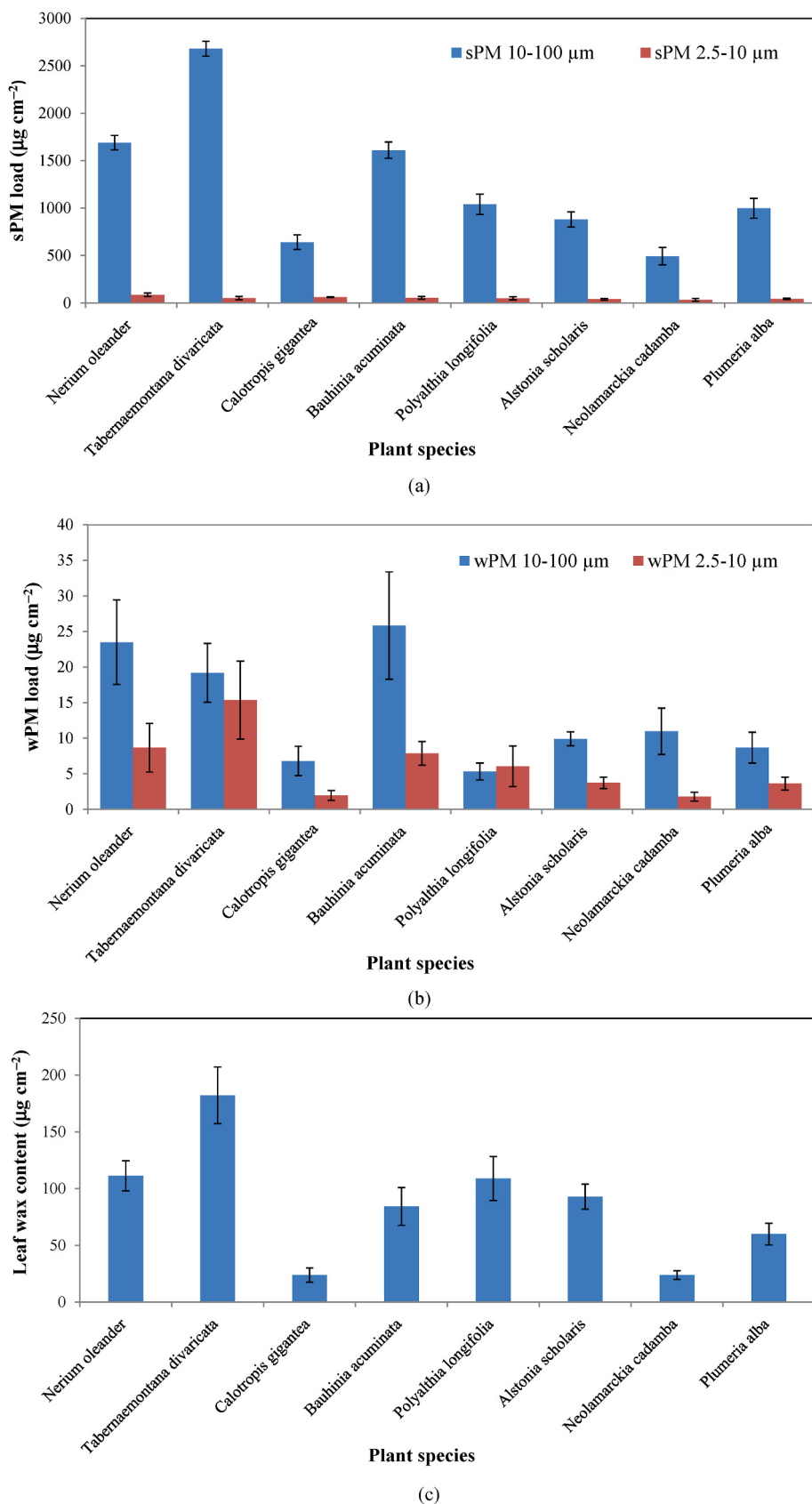


Fig. 2. Foliar contents ($\mu\text{g cm}^{-2}$) of (a) surface PM (sPM), (b) wax PM (wPM) of different size fractions and (c) waxes of selected plant species (data are presented as mean \pm SD, $n = 3$).

affecting the flow regime of ambient air and cause swaying, bending and fluttering of leaves through absorption of wind momentum and dissipation of energy due to eddy shedding and formation of turbulence within the plants, resulting in deposition or dislodging of particulates (Gemba, 2007; Gillies et al., 2002). Based on the inferences given by Corada et al. (2021), Leonard et al. (2016), Popek et al. (2013), Przybysz et al. (2014), Saebo et al. (2012) and Weerakkody et al. (2018), it has become increasingly evident that the lanceolate, ovate, obovate and lobed leaves are more capable of capturing particles. *T. divaricata*,

N. oleander and *B. acuminata* exhibited high PM capturing potential because of their short/medium height, bushy nature and spreading crown with dense leaf arrangement; deposition being also greatly effected by their leaf shapes — lanceolate, linear-lanceolate and bilobed ovate respectively. *P. longifolia* (ovate-lanceolate leaves with wavy margin), *P. alba* (obovate leaves) and *A. scholaris* (narrowly obovate leaves) were also found to be good accumulators of PM owing to their complex leaf shape. *C. gigantea* (elliptic-ovate leaves), though of medium height, did not show much potential for PM capturing. *N. cadamba*

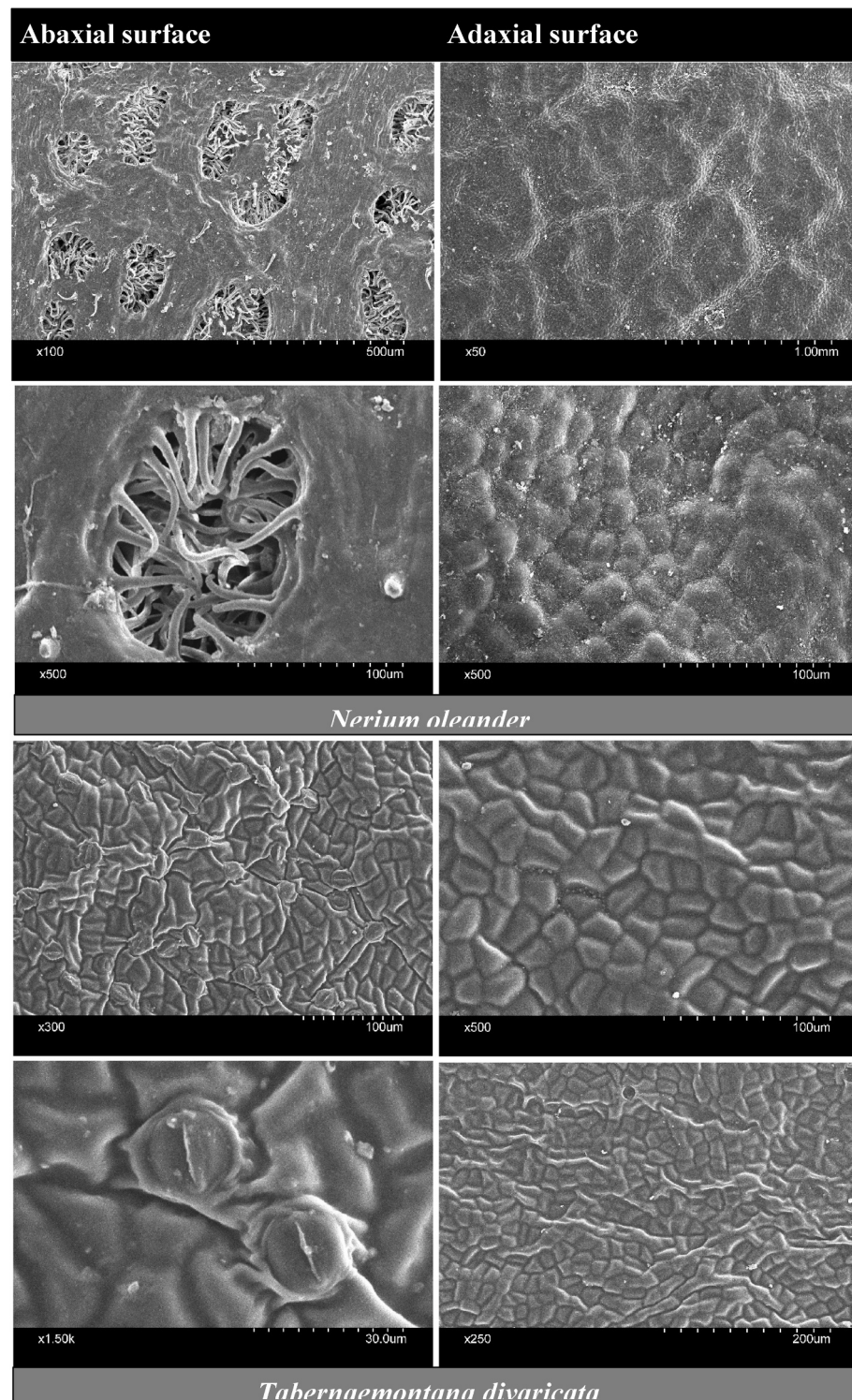


Fig. 3. SEM images of abaxial and adaxial surfaces of studied plant leaves with particulate deposition.

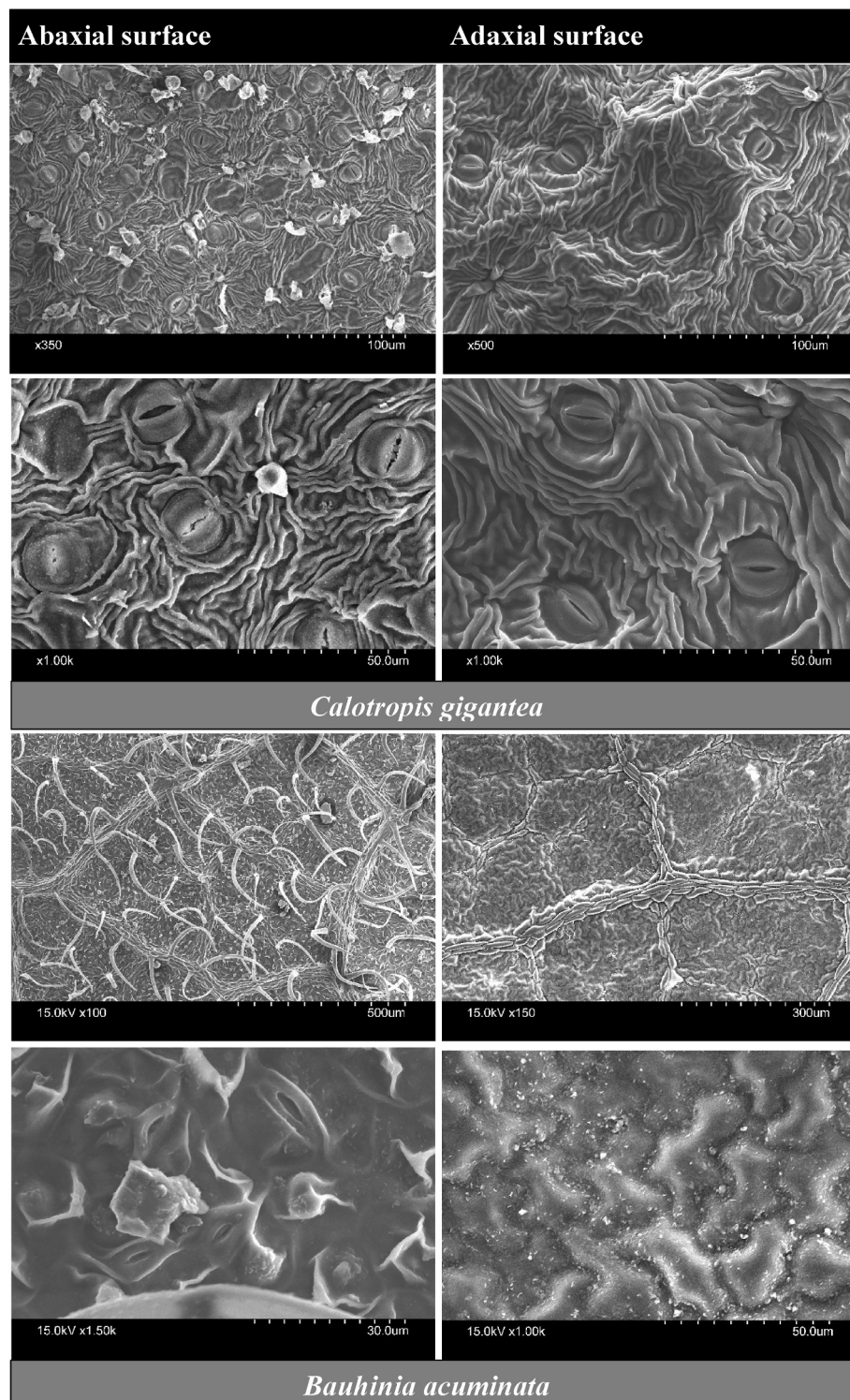


Fig. 3. (continued).

(elliptic-oblong to ovate leaves) was least effective in PM retention due to its large height and branched nature. Similarly, Chowdhury et al. (2022) indicated an inverse relationship between foliar deposition of PM and increased height of urban trees. Moreover, peculiar elliptical shapes of *C. gigantea* and *N. cadamba* leaves were not very much conducive to the retention of PM as already explained by Leonard et al. (2016) and Weerakkody et al. (2018). Although noticeable PM accumulation per square cm of leaf area was not achieved for these two species in contrast to others, as a whole they can very well be used for green belts as

filtering barriers against pollution and phytoaccumulators, ensuring ecological balance (Pragasan and Ganesan, 2022; Sharma and Tripathi, 2009). They also have their ornamental values and economic consideration in India.

Efficacies of evergreen plants for the interception of large quantities of PM have been documented in several studies because of their strong abilities of foliage retention and typical leaf morphology (Cai et al., 2017; Corada et al., 2021; Zhou et al., 2022). However, in the proposed work, *B. acuminata* and *P. alba*, though deciduous species, performed

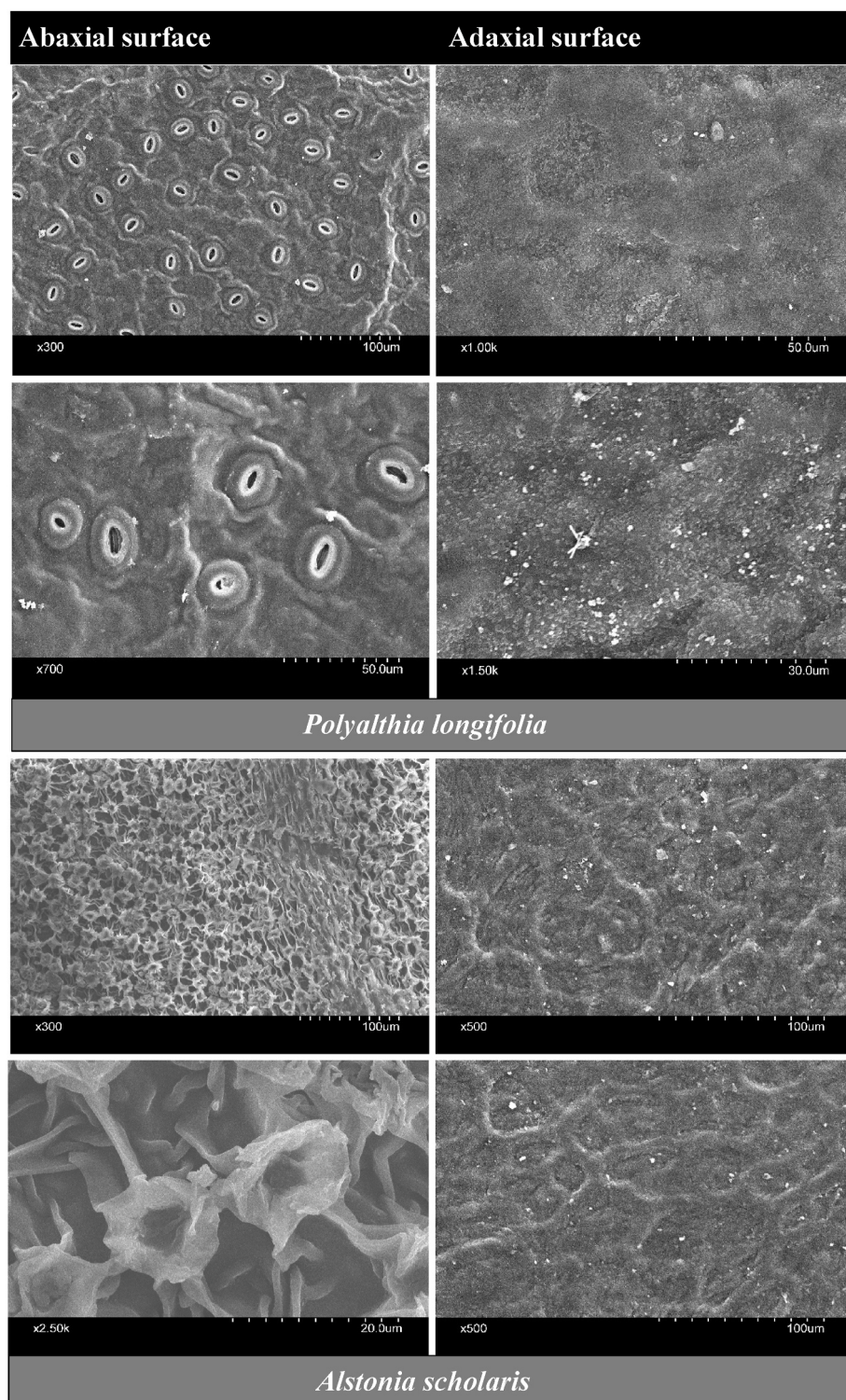


Fig. 3. (continued).

desirably well to capture PM besides the other evergreen ones. Reduction in the ambient concentrations of PM by about 60% was achieved by Pugh et al. (2012) using deciduous trees and shrubs in the urban areas of street canyons. Lukowski et al. (2020) proved that the leaf surfaces of deciduous species, *B. pendula* and *Q. robur*, were highly retentive in capturing PM and *B. pendula*, being the best performer, can be effectively utilized for planting in urban environment in order to improve roadside air quality. Thus, application of deciduous plants should also be highlighted for the development of green infrastructure-based ambient

air pollution control system (i.e. passive control) in combination with evergreen species.

Leaf surface microstructure is one of the key factors associated with plant species' ability for adsorption or absorption of PM. The differences in the micromorphology of abaxial and adaxial surfaces of the plant leaves are apparent from Fig. 3. *T. divaricata*, *C. gigantea* and *P. alba* manifested greater number of stomata on the abaxial surface than that of the adaxial side, whereas, no occurrence of stomata was noted in the adaxial surfaces of *B. acuminata*, *P. longifolia* and *N. cadamba*, but, high

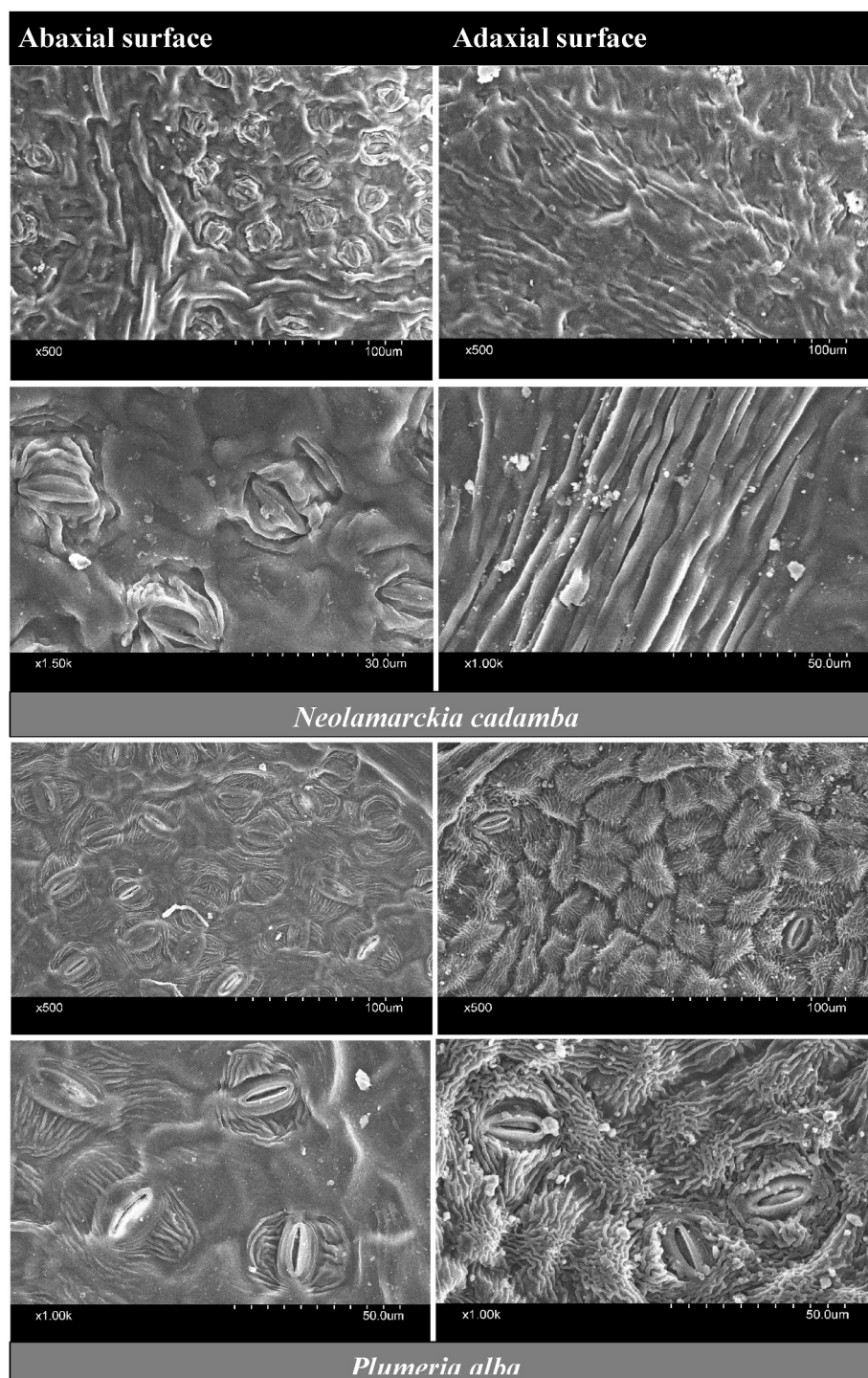


Fig. 3. (continued).

stomatal count was noticed in the abaxial surfaces of the same. However, open and closed stomatal distribution across the leaf epidermis caused heterogeneity in the areas of stomatal pores, influencing PM deposition through developed creases. The abaxial side of *N. oleander* was found to be characterized with highly cutinized epidermis having multiple layers and many large depressions (crypts) with prominently distributed trichomes or leaf hairs, densely covering, lining and projecting into the epidermal cavities and guarding the stomata within the crypts, thereby promoting PM capture (Stefi et al., 2020). Adaxial epidermis showed convex epidermal cell patterns with wax platelets forming roughness on the surfaces which helped accumulation of

particulates in the grooves and furrows (Adhikari et al., 2021). The upper and lower epidermis of *T. divaricata* revealed the presence of a compact organization of epidermal cell lining combined with cuticular covering, leading to a grooved or striated surface (Seenu et al., 2019). Such intricate networks of leaf surface topography facilitated highest particle deposition. In *C. gigantea*, cuticular striations were present around the stomata, spreading out covering guard cells and epidermal cells on both upper and lower sides of the leaves, having particles sticking to the stomatal openings and the adjoining clefts, rifts or narrow grooves generated by the clustering of waxy cuticular materials (Abey-singhe and Scharaschkin, 2022). The adaxial epidermal surface of

N. cadamba consisted of wrinkled and striated dense cuticular protrusions or ridges, but, on the abaxial surface, the same were detected surrounding the stomata (Jamil et al., 2009). Despite the presence of uneven microstructures with ridges or grooves, foliar accumulation of PM on the leaves of *C. gigantea* and *N. cadamba* was not significantly appreciable in respect of other species. Therefore, it can be presumed that the large leaf size, elliptic shape, arrangement and field/environmental conditions may also act as limiting factors for PM capture (Leonard et al., 2016). Additionally, plant height sometimes plays an important role. The epidermis of *B. acuminata* contained large number of abaxial trichomes protruding from fibrous midrib, veins and veinlets,

creating deep ridges and irregular polygonal convex shaped adaxial epidermal cells forming trenches and grooves. These particular morphological structures assisted in huge PM accumulation (Duartte-Almeida et al., 2015; Pereira et al., 2018). It is well-known that the leaf hairs reduce the rate of retained particulate resuspension and provide high surface area for capture, enhancing foliage adhesion of particles (Leonard et al., 2016; Prusty et al., 2005; Qiu et al., 2009; Saebo et al., 2012). A huge number of stomata were seen in the lower epidermis of *P. longifolia* with particle deposition in and around the stomatal cavities. It has been seen in *P. longifolia* that the high stomatal conductance increases the rate of transpiration in plants, accelerating

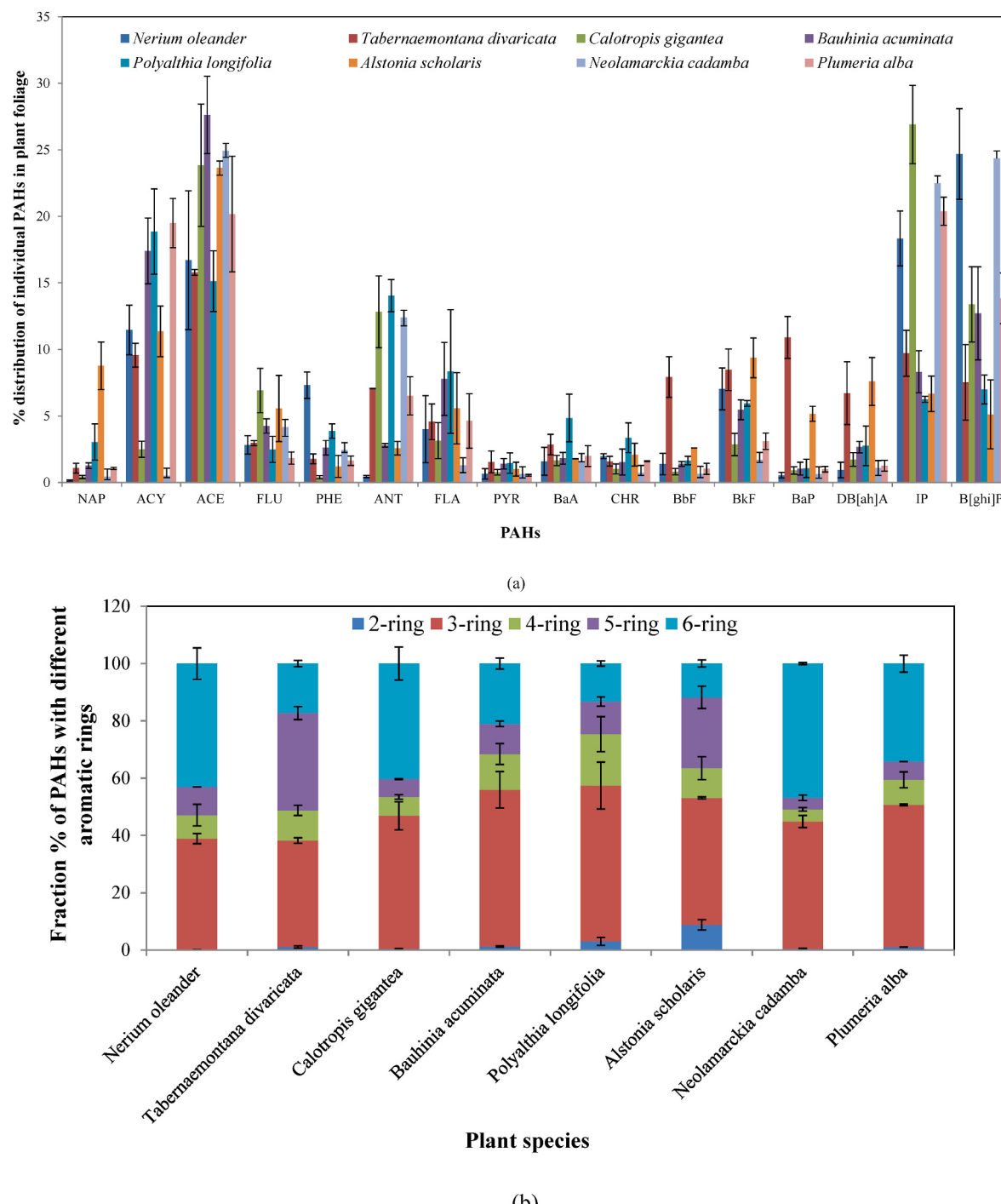


Fig. 4. Variations in leaf accumulation (mean \pm SD, n = 3) of PAHs in plant species (a) % distribution of individual PAHs and (b) % fraction of PAHs of different aromatic rings with respect to total PAHs.

the capture of PM on the moisture layer formed due to transpiration (Jamil et al., 2009; Tong, 1991). The adaxial surface, on the other hand, also indicated particulate accumulation on the waxy film of the epidermis. In *A. scholaris*, the cuticular layer appeared to be in varicose and papillate forms with cuticular ridges interconnecting the projections on the abaxial epidermis, hiding the stomata underneath. Perhaps, such morphology might have been resulted from the species' response to biotic/abiotic stress to thrive in the polluted environment and aided the entrapment of particles in the protrusions, inhibiting their entry into the hidden stomatal apparatus and clogging thereof. Polygonal epidermal cell outlines having striated cuticles were observed on the adaxial side with particle deposition (Singh et al., 2016). The upper and lower epidermal surfaces of *P. alba* leaves are composed of cuticular layer with arch like structures, paracytic stomata (embedded within cuticular arches), vein-like projections and cell lining, developing grooves and ridges which might be associated with PM retention (El-Khatib et al., 2012; Shrivastava and Mishra, 2018). Studies carried out by Li et al. (2021), Niu et al. (2020), Redondo-Bermudez et al. (2021), Shao et al. (2019) and Weerakkody et al. (2018) also corroborated the current observations, explicitly elaborating the importance of plant leaves with rough surfaces, microhairs, epidermal undulations due to specialized cell structure, distinct stomatal complexes, cuticular folds and waxes.

3.2. Bioaccumulation of PAHs

It is an established fact that the foliar uptake is the principal route of PAHs transfer directly from the atmosphere to the plants when exposed to airborne PAHs pollution in the outdoor environment (Lehndorff and Schwark, 2004). PAHs may either be adsorbed on waxy cuticular leaf surfaces or absorbed in the internal leaf mesophyll tissues (penetrating the membranes) via cuticular and stomatal infiltration (Desalme et al., 2013). Interspecies variations in the pattern of accumulation of PAHs in plant leaves relating to the distribution percentage of each foliar PAH congener and contribution percentage of PAHs categorized by different aromatic rings to total PAHs are evaluated based on the PAHs concentrations in the samples and represented in Fig. 4a and b. Significant differences were found in the accumulated concentrations of PAHs among the species using two-way ANOVA ($F > F_{crit}$ and $p < 0.05$). Proportion of HMW PAHs (4–6 rings) was found to be higher with respect to LMW PAHs (2–3 rings) in *N. oleander* (~61%), *T. divaricata* (~62%), *C. gigantea* (~53%) and *N. cadamba* (~55%), whereas in *P. alba*, the difference is marginal (LMW: ~51% and HMW: ~49%). Besides, *B. acuminata*, *P. longifolia* and *A. scholaris* showed greater potential for accumulation of LMW PAHs (~56%, ~57% and ~53% respectively). ACY, ACE, IP and B[ghi]P appeared to be the high yielding compounds in the leaves of *N. oleander*, *B. acuminata* and *P. alba* with 11.46–19.49%, 16.71–27.63%, 8.32–20.38% and 12.71–24.69% contributions respectively (ref. Fig. 4a). A similar distribution pattern of PAHs was observed in *C. gigantea* and *N. cadamba* exhibiting high levels of ACE, ANT, IP and B[ghi]P (~77% and 84% of total PAHs respectively). Highest proportion of BaP (a potent carcinogen) was noted in *Tabernaemontana* leaves (10.90% vs. other species: 0.54–5.16%) with PAHs, such as ACY, ACE, BkF and IP also having higher percentage compositions. Relative abundance of ACY and ACE followed by ANT and FLA in *P. longifolia* (18.86%, 15.13%, 14.04% and 8.34% respectively) and BkF and NAP in *A. scholaris* (11.36%, 23.63%, 9.37% and 8.77% respectively) was also evident from experimental observation. Thus, as seen from Fig. 4b, percentage of 3-ring PAHs (~37–55%) was highest in almost all the species except *N. oleander* (~43%) and *N. cadamba* (~47%) where 6-ring PAHs were dominant. However, for the two species, percentage composition of PAHs with 3-rings was detected as ~39% and ~44% respectively. *C. gigantea* (~40%) and *P. alba* (~34%) were also able to arrest high proportion of 6-ring PAHs when compared with *T. divaricata* (~17%), *B. acuminata* (~21%), *P. longifolia* (~13%) and *A. scholaris* (~12%). 4-ring compounds accounted for ~4–18% of the total PAHs in the leaves of studied plants. Concerning 5-ring PAHs,

T. divaricata showed highest fraction percentage (~34%) followed by *A. scholaris* (~25%) and least in *N. cadamba* (~4%). Contribution of 2-ring congener (NAP) to total PAHs was considerably low, ranging between ~0.13 and 9% in the plant species, which may be attributed to its high volatility and degradability. The mechanism of PAHs accumulation is mainly effected by gaseous diffusion and deposition based on equilibrium partitioning and gas-phase kinetics respectively, along with wet and dry deposition of PAHs associated with particles. Such processes are frequently controlled by man-made impacts, ambient concentration levels, meteorology, climatology, ecosystem properties and characteristics of plant surfaces (leaf hair density, roughness, texture, wettability and structural features of epidermis) (Desalme et al., 2013; Loppi et al., 2015). Since, leaf morphology differs greatly with plant diversity, accumulation behaviour is species-specific. All these factors caused differences in PAHs bioavailability, composition and content in the leaves of individual plant species from even proximal areas (Gerdol et al., 2002). Numerous studies have investigated airborne PAHs–leaf interactions in many plants and reported differential accumulation patterns of PAHs based on the species, thereby stating it a complex phenomenon (Jia et al., 2019; Pleijel et al., 2022; Tian et al., 2019; Yang et al., 2017). In the current study, the trend of total concentration ($\mu\text{g g}^{-1}$ DW) of PAHs in the plant samples was determined as: *T. divaricata* (393.01 ± 30.34) > *P. alba* (342.28 ± 25.38) > *N. cadamba* (301.13 ± 37.31) > *N. oleander* (286.08 ± 32.65) > *C. gigantea* (267.47 ± 11.49) > *A. scholaris* (256.80 ± 32.31) > *B. acuminata* (177.22 ± 14.57) > *P. longifolia* (159.92 ± 21.23). SLA ($\text{cm}^2 \text{g}^{-1}$) of plants, which has an important bearing on the accumulation of PAHs through foliage and reflects the leaf surface area available per unit mass for the uptake of pollutants from ambient air (Nizzetto et al. (2008)), varied in the following order: *T. divaricata* (376.79 ± 0.74) > *B. acuminata* (190.82 ± 0.91) > *P. longifolia* (150.82 ± 0.49) > *C. gigantea* (138.47 ± 0.21) > *P. alba* (136.45 ± 0.55) > *N. cadamba* (131.34 ± 0.29) > *A. scholaris* (122.16 ± 0.19) > *N. oleander* (71.01 ± 0.47). A positive correlation was observed between SLAs and accumulated PAHs levels ($r = 0.42$, $p < 0.05$), which indicated that the SLA would favour the process of foliar absorption of PAHs, depending also on other morphological factors. Positive influence of SLA on PAHs concentrations was again suggested by Terzaghi et al. (2015) and Wang et al. (2020). Leaf concentrations of PAHs were found to be weakly related ($r = 0.35$, $p < 0.05$) to total PM load, which may be due to different independent sources of emission affecting their deposition.

The concentrations of PAH compounds can be employed for the recognition of their emission source types. In this context, a total index (TI) was applied to distinguish between PAHs originated from high (TI > 4) and low (TI < 4) temperature processes. The TI is generally given by the following formula (Orecchio, 2010):

$$TI = \frac{FLA}{(FLA + PYR) \times 0.4} + \frac{ANT}{(ANT + PHE) \times 0.1} + \frac{BaA}{(BaA + CHR) \times 0.2} \\ + \frac{IP}{(IP + B[ghi]P) \times 0.2} \quad (11)$$

TI values for all the plant samples were estimated as follows: *N. oleander* (7.08 ± 0.94), *T. divaricata* (15.89 ± 1.68), *C. gigantea* (18.16 ± 0.58), *B. acuminata* (11.97 ± 0.62), *P. longifolia* (15.29 ± 1.15), *A. scholaris* (14.07 ± 2.88), *N. cadamba* (15.90 ± 0.36) and *P. alba* (15.98 ± 0.54) and found to be more than 4, signifying vehicular emission (i.e. high temperature combustion) as the major source of PAHs in the study area. Liu et al. (2017), Pereira et al. (2019) and Pu et al. (2022) have used TI for identifying the sources of PAHs contamination in surface soil and subsoil layers of different depths, tree barks, total suspended particles as well as gas-phase samples and found the predominance of combustion-derived PAHs. Accretion of carcinogenic PAHs of high molecular weight (viz. BaA, CHR, BbF, BaP, DB[ah]A and IP) as shown in the present work elucidates the importance of the

selected species for biomonitoring studies. Therefore, natural vegetation with vast accumulating surfaces is crucially important in urban landscapes for scavenging or removing PAHs from the atmosphere and creates an ambience of biomonitoring of cumulative impacts of PAHs pollution using plant leaves, so vital for environmental quality assessment.

3.3. Carcinogenic and mutagenic risks of PAHs

The carcinogenicity and mutagenicity of foliar PAHs were investigated in the present study in the context of BaP equivalent concentrations (BaP_{TEQ} and BaP_{MEQ}), CP and MP to represent the toxicity of PAHs. Two-way ANOVA showed statistically significant differences ($F > F_{crit}$ and $p < 0.05$) among the concentrations, CP and MP for all the species. ΣBaP_{TEQ16} (sum total of carcinogenic or toxic equivalent concentrations of 16 PAHs) and ΣBaP_{MEQ8} (sum total of mutagenic equivalent concentrations of 8 PAHs) were found to be in the range of 9.51 ± 1.73 – 81.37 ± 5.35 and 10.60 ± 0.09 – $80.42 \pm 11.44 \mu\text{g g}^{-1}$ respectively for all the selected species (ref. Table 2a and Table 2b). Major contribution (91.54–99.12%) of seven carcinogenic PAHs having 4-, 5- and 6-rings, as mentioned earlier, was detected with the dominance of BkF, BaP, DB[ah]A and IP, which catered to the maximum toxicity in relation to ΣBaP_{TEQ16} . In case of ΣBaP_{MEQ8} , highest mutagenic threats were posed by 5- and 6-ring PAHs accounting for 93.21–98.90% among the plant species. Moreover, it can be seen from Table 2c that the 4–6 ring PAHs have highest CP, whereas, 5–6 ring PAHs indicated high mutagenicity (i.e. high MP, ref. Table 2d). Vehicular sources (i.e. emissions from fuel vehicles powered by petrol, diesel, natural gas or local blending of petrol with kerosene oil) might be the root cause for the release of carcinogenic and mutagenic PAHs in the sampling locations. Based on the above findings, it can be opined that the assessment and control of HMW PAHs should be given utmost priority for maintaining a clean and habitable environment and reducing possible health risks. Evaluation of potential risks of PAHs for hazard analysis due to exposure has been actively performed by many researchers (Blaszczyk et al., 2017; Fred-Ahmadu and Benson, 2019; Ihunwo et al., 2021; Li et al., 2014) which is quite compatible with the results of the current study.

3.4. Analysis of biomarkers and pollution/performance indices for comparing the suitability of plant species for urban plantation

Leaf biomarkers, APTI and API, based on the characterization of plants, have been used to discern the functioning of terrestrial plants in response to prevailing pollutant changes for increasing vegetation coverage along the urban streets for uplifting the quality of ambient air. The statistical comparison of leaf characteristics and indices by two-way ANOVA revealed significant differences ($F > F_{crit}$ and $p < 0.05$) among the species.

3.4.1. Contents of photosynthetic pigments (chlorophyll (Chl) and carotenoids ($C_X + C$))

Chlorophyll and carotenoids are the key functional pigments of plants which control the photosynthetic capacity, favouring plant growth and yield. In response to abiotic stress, plants induce adaptive changes in their leaf traits to cope up with the environmental fluctuations. Likewise, plants are able to modulate the levels of required pigments and acclimatize to the surrounding environment for maintaining the normal process of photosynthesis (Li et al., 2018). The results demonstrated that the values of Chl_T, Chl a/b and $C_X + C$ varied from 0.90 to 5.13 mg g⁻¹, 1.73–4.23 mg g⁻¹ and 0.24–1.12 mg g⁻¹ respectively (ref. Table 3). It is also apparent from Table 3 that the values of Chl a are higher than Chl b for all the plants considered. Both Chl_T and $C_X + C$ differed widely among plant species: a) shrubs: Chl_T (*T. divaricata*) > Chl_T (*C. gigantea*) > Chl_T (*P. alba*) > Chl_T (*B. acuminata*) > Chl_T (*N. oleander*); $C_X + C$ (*T. divaricata*) > $C_X + C$ (*C. gigantea*) > $C_X + C$ (*B. acuminata*) > $C_X + C$ (*P. alba*) > $C_X + C$ (*N. oleander*) and b) trees: Chl_T (*N. cadamba*) > Chl_T (*P. longifolia*)

Table 2(a)
Toxic equivalent concentrations (TEQ) of PAHs accumulated in the leaves of selected plant species.

PAHs	TEQ ^a	BaP _{TEQ} (μg g ⁻¹) (mean ± SD) of PAHs						
		<i>Nerium oleander</i>	<i>Tabernaemontana divaricata</i>	<i>Calotropis gigantea</i>	<i>Bauhinia acuminata</i>	<i>Polyalthia longifolia</i>	<i>Alstonia scholaris</i>	<i>Neolamarckia cadamba</i>
NAP	0.001	0.0004 ± 0.0002	0.004 ± 0.001	0.001 ± 0.0003	0.002 ± 0.0004	0.005 ± 0.001	0.002 ± 0.005	0.001 ± 0.001
ACY	0.001	0.03 ± 0.01	0.04 ± 0.01	0.007 ± 0.002	0.03 ± 0.01	0.03 ± 0.01	0.03 ± 0.01	0.07 ± 0.01
ACE	0.001	0.05 ± 0.01	0.06 ± 0.004	0.05 ± 0.01	0.05 ± 0.01	0.02 ± 0.003	0.06 ± 0.01	0.07 ± 0.01
FLU	0.001	0.008 ± 0.003	0.01 ± 0.004	0.02 ± 0.01	0.004 ± 0.002	0.01 ± 0.002	0.01 ± 0.001	0.006 ± 0.002
PHE	0.001	0.02 ± 0.01	0.007 ± 0.001	0.001 ± 0.0003	0.005 ± 0.002	0.006 ± 0.001	0.003 ± 0.001	0.007 ± 0.001
ANT	0.01	0.01 ± 0.002	0.28 ± 0.02	0.34 ± 0.06	0.05 ± 0.002	0.22 ± 0.04	0.07 ± 0.02	0.37 ± 0.06
FLA	0.001	0.01 ± 0.01	0.02 ± 0.002	0.008 ± 0.003	0.01 ± 0.01	0.01 ± 0.01	0.01 ± 0.01	0.004 ± 0.001
PYR	0.001	0.002 ± 0.0003	0.006 ± 0.003	0.002 ± 0.0004	0.002 ± 0.0001	0.002 ± 0.0001	0.003 ± 0.0005	0.002 ± 0.0004
BaA	0.10	0.45 ± 0.20	1.12 ± 0.36	0.44 ± 0.12	0.32 ± 0.09	0.77 ± 0.13	0.46 ± 0.06	0.49 ± 0.08
CHR	0.01	0.45 ± 0.20	1.12 ± 0.36	0.44 ± 0.12	0.32 ± 0.09	0.77 ± 0.13	0.46 ± 0.06	0.49 ± 0.08
BbF	0.10	0.39 ± 0.15	1.12 ± 0.78	0.32 ± 0.01	0.03 ± 0.01	0.05 ± 0.02	0.05 ± 0.01	0.02 ± 0.01
BkF	0.10	2.01 ± 0.61	3.33 ± 0.81	0.76 ± 0.24	0.97 ± 0.04	0.95 ± 0.15	2.41 ± 0.62	0.51 ± 0.11
BaP	1.00	1.55 ± 0.30	42.84 ± 8.80	2.42 ± 0.59	1.82 ± 0.61	1.68 ± 0.66	13.25 ± 2.84	1.86 ± 0.52
DB[ah]A	1.00	2.66 ± 1.09	4.61 ± 1.08	4.69 ± 1.06	4.40 ± 1.35	4.40 ± 1.35	19.50 ± 6.27	3.26 ± 0.98
IP	0.10	5.25 ± 1.99	7.19 ± 1.04	1.48 ± 0.37	0.99 ± 0.09	1.71 ± 0.49	1.71 ± 0.49	6.77 ± 0.69
BighillP	0.01	0.71 ± 0.17	0.29 ± 0.08	0.36 ± 0.09	0.23 ± 0.03	0.11 ± 0.03	0.13 ± 0.04	0.73 ± 0.09
ΣBaP_{TEQ16}	–	13.21 ± 0.13	81.37 ± 5.35	16.47 ± 0.28	9.95 ± 0.85	9.51 ± 1.73	38.39 ± 10.36	14.31 ± 0.49
								17.69 ± 0.96

^a List proposed by Nisbet and LaGoy (1992).

Table 2(b)
Mutagenic equivalent concentrations (MEQ) of foliar PAHs.

PAHs	MEF ^a	<i>Nerium oleander</i>	<i>Tabernaemontana divaricata</i>	<i>Calotropis gigantea</i>	<i>Bauhinia acuminata</i>	<i>Polyalthia longifolia</i>	<i>Astonia scholaris</i>	<i>Neolamarckia cadamba</i>	<i>Plumeria alba</i>
BaA	0.082	0.37 ± 0.16	0.92 ± 0.29	0.36 ± 0.09	0.26 ± 0.08	0.63 ± 0.11	0.37 ± 0.05	0.39 ± 0.06	0.56 ± 0.15
CHR	0.017	0.09 ± 0.01	0.11 ± 0.01	0.05 ± 0.02	0.05 ± 0.02	0.09 ± 0.04	0.09 ± 0.02	0.04 ± 0.01	0.09 ± 0.01
BbF	0.25	0.99 ± 0.37	7.79 ± 1.94	0.54 ± 0.13	0.62 ± 0.02	0.66 ± 0.19	1.67 ± 0.22	0.49 ± 0.11	0.87 ± 0.26
BkF	0.11	2.21 ± 0.66	3.66 ± 0.88	0.84 ± 0.27	1.06 ± 0.04	1.05 ± 0.17	2.65 ± 0.69	0.56 ± 0.12	1.16 ± 0.29
BaP	1.0	1.55 ± 0.30	42.84 ± 8.80	2.42 ± 0.59	1.82 ± 0.61	1.68 ± 0.66	13.25 ± 2.84	1.86 ± 0.52	3.42 ± 0.93
DBfahIA	0.29	0.77 ± 0.32	7.64 ± 1.81	1.34 ± 0.31	1.36 ± 0.30	1.28 ± 0.39	5.66 ± 1.82	0.95 ± 0.28	1.24 ± 0.28
IP	0.31	16.26 ± 3.39	11.84 ± 2.80	22.31 ± 3.25	4.57 ± 1.14	3.09 ± 0.32	5.30 ± 1.53	20.99 ± 2.13	21.63 ± 2.62
BghiJP	0.19	13.42 ± 3.08	5.62 ± 1.46	6.79 ± 1.63	4.28 ± 0.69	2.12 ± 0.55	2.49 ± 0.74	13.94 ± 1.85	8.99 ± 1.77
Σ BaP _{MEQ}	—	35.66 ± 5.99	80.42 ± 11.44	34.65 ± 4.24	14.02 ± 0.14	10.60 ± 0.09	31.48 ± 6.39	39.22 ± 3.25	37.96 ± 4.93

^a List proposed by Durant et al. (1996).

> Chl_T (*A. scholaris*); C_{X + C} (*P. longifolia*) > C_{X + C} (*N. cadamba*) > C_{X + C} (*A. scholaris*). It was observed by many researchers that in presence of PM pollution, Chl a/b ratio reduced owing to the shading of leaves by the particulate-induced decrease in the penetration of incident light (Nanos and Ilias, 2007; Shabnam et al., 2021). It is also consistent with the present study as a negative correlation ($r = -0.46$, $p < 0.05$) was obtained between total PM load and Chl a/b ratio. The changes in the ratio might be an indication of the adaptive nature of plant leaves for maximization of the photosynthetic performance towards varying intensities of light, thereby controlling the concentration and composition of Chl molecules as well as the main functional units, photosystems I and II; the low values of Chl a/b being responsible for enhancing the light absorption capacity under PM stress (Porra and Scheer, 2019; Shabnam et al., 2015, 2021). Moreover, C_{X + c} and Chl_T were found to be positively correlated to each other ($r = 0.83$, $p < 0.05$) which may be attributed to the antioxidant activity of carotenoids in safeguarding the chloroplasts for retaining higher chlorophyll concentration (Kacharava et al., 2009). High levels of leaf Chl_T were noted for species *T. divaricata*, *C. gigantea*, *N. cadamba* and *P. alba*. Substantially high concentrations of chlorophyll and carotenoids can effectively be linked to the tolerance of plants against stress as already established in different studies (Enete et al., 2013; Ogunkunle et al., 2015).

3.4.2. Ascorbic acid (AA) content

AA, the non-enzymatic antioxidant, is an essential metabolite of plant leaves associated with the stress response to multiple interacting factors (abiotic or biotic stressors), which upregulates many metabolic functions in plants for developing their tolerance against environmental adversity (Pathak et al., 2019). Furthermore, it is able to quench or eliminate the increased levels of reactive oxygen species (ROS) generated due to pollutant exposure in the plant cells either directly or by functioning through enzymatic reactions involved in ascorbate-glutathione pathway. Thus, it upholds the equilibrium in between generation and mitigation of ROS (Frei et al., 2012). In the plant leaves, AA contents ranged from 3.63 to 18 mg g⁻¹ as indicated in Table 3. Positive correlations were observed between AA contents and total PM ($r = 0.64$, $p < 0.05$) and PAHs ($r = 0.84$, $p < 0.05$) loads, justifying the presumption of the increase in leaf AA with abiotic stress. Plants having higher concentrations of AA (in this case: *T. divaricata*, *N. oleander* and *P. alba*) are said to develop more tolerance enabling them to respond quickly to pollutants for their survival and growth. However, *B. acuminata*, *P. longifolia* and *A. scholaris* exhibited lower levels of AA — this may be due to the fact that the production of AA got hampered, rendering them slow respondent towards detoxification of ROS or oxidative damage (Shah et al., 2020). The remaining two species, *C. gigantea* and *N. cadamba*, synthesized and maintained an intermediate level of AA to counter the phytotoxic effects of pollutants. The present findings revealed good congruence with recent researches (Banerjee et al., 2022; Goswami et al., 2023).

3.4.3. Foliar pH

Leaf extract pH serves as a stress biomarker directing pivotal functions, such as biochemical and physiological activities along with the processes of homeostatic control in plant cells (Mandal and Dhal, 2022). It has been noticed that the range of leaf pH in the collected species lies between 5.91 and 7.47 (Table 3). As illustrated in previous case studies (Escobedo et al., 2008; Govindaraju et al., 2012; Singh et al., 2023), plants exhibiting high foliar pH values (close to 7 or greater) are known to acquire stress tolerance to a considerable extent, which may be linked to higher endogenous biosynthesis of AA in plants from hexose sugars imparting good resilience to fight against environmental pollution. This was corroborated by the positive correlation ($r = 0.94$, $p < 0.05$) as obtained between leaf pH and AA levels and also conformed to the results of Zhang et al. (2020). Contrariwise, air pollution sensitivity across species increases with lower pH (formed as a result of plant metabolic alterations through stomatal uptake of polluting gases (e.g. nitrogen

Table 2(c)

Carcinogenic potential (CP) of accumulated PAHs in the plant leaves.

PAHs	CP (in %) (mean ± SD)							
	<i>Nerium oleander</i>	<i>Tabernaemontana divaricata</i>	<i>Calotropis gigantea</i>	<i>Bauhinia acuminata</i>	<i>Polyalthia longifolia</i>	<i>Alstonia scholaris</i>	<i>Neolamarckia cadamba</i>	<i>Plumeria alba</i>
NAP	0.002 ± 0.001	0.01 ± 0.002	0.01 ± 0.005	0.02 ± 0.002	0.05 ± 0.003	0.06 ± 0.003	0.01 ± 0.002	0.02 ± 0.002
ACY	0.23 ± 0.05	0.05 ± 0.01	0.04 ± 0.01	0.31 ± 0.04	0.32 ± 0.12	0.08 ± 0.002	0.01 ± 0.003	0.38 ± 0.04
ACE	0.35 ± 0.07	0.08 ± 0.005	0.39 ± 0.04	0.49 ± 0.05	0.25 ± 0.09	0.16 ± 0.03	0.52 ± 0.08	0.39 ± 0.07
FLU	0.06 ± 0.02	0.01 ± 0.002	0.11 ± 0.03	0.08 ± 0.01	0.04 ± 0.02	0.04 ± 0.03	0.09 ± 0.03	0.04 ± 0.01
PHE	0.12 ± 0.01	0.01 ± 0.001	0.01 ± 0.005	0.05 ± 0.01	0.06 ± 0.02	0.01 ± 0.01	0.05 ± 0.01	0.03 ± 0.01
ANT	0.10 ± 0.001	0.34 ± 0.004	2.08 ± 0.28	0.5 ± 0.02	2.35 ± 0.71	0.17 ± 0.004	2.61 ± 0.49	1.26 ± 0.29
FLA	0.08 ± 0.04	0.02 ± 0.01	0.05 ± 0.02	0.14 ± 0.05	0.14 ± 0.02	0.04 ± 0.03	0.03 ± 0.003	0.09 ± 0.04
PYR	0.01 ± 0.01	0.01 ± 0.002	0.01 ± 0.004	0.02 ± 0.01	0.02 ± 0.01	0.01 ± 0.004	0.01 ± 0.01	0.01 ± 0.001
BaA	3.40 ± 1.59	1.37 ± 0.38	2.67 ± 0.74	3.22 ± 0.77	8.10 ± 0.05	1.19 ± 0.26	3.39 ± 0.62	3.83 ± 1.38
CHR	0.47 ± 0.11	0.08 ± 0.01	0.16 ± 0.06	0.27 ± 0.18	0.56 ± 0.26	0.14 ± 0.11	0.15 ± 0.05	0.31 ± 0.004
BbF	3.05 ± 1.13	3.83 ± 0.77	1.32 ± 0.27	2.49 ± 0.32	2.75 ± 1.03	1.73 ± 0.39	1.37 ± 0.25	1.97 ± 0.76
BkF	15.14 ± 4.45	4.09 ± 0.79	4.63 ± 1.52	9.75 ± 1.36	9.96 ± 2.71	6.27 ± 0.13	3.56 ± 0.85	5.98 ± 1.29
BaP	11.74 ± 2.45	52.65 ± 8.11	14.69 ± 3.28	18.32 ± 8.71	17.61 ± 3.05	34.51 ± 3.10	13.00 ± 3.06	19.34 ± 4.54
DB[ah]	20.18 ± 8.54	32.40 ± 10.79	27.98 ± 5.95	47.22 ± 7.61	46.12 ± 4.73	50.79 ± 4.24	22.77 ± 5.76	24.21 ± 7.22
A								
IP	39.67 ± 7.97	4.69 ± 0.88	43.68 ± 6.94	14.85 ± 2.79	10.50 ± 2.38	4.46 ± 0.15	47.31 ± 6.13	39.46 ± 2.85
B[ghi]P	5.40 ± 1.23	0.36 ± 0.13	2.17 ± 0.55	2.27 ± 0.63	1.17 ± 0.41	0.34 ± 0.31	5.12 ± 0.81	2.68 ± 0.42

Table 2(d)

Mutagenic potential (MP) of accumulated PAHs in the plant leaves.

PAHs	MP (in %) (mean ± SD)							
	<i>Nerium oleander</i>	<i>Tabernaemontana divaricata</i>	<i>Calotropis gigantea</i>	<i>Bauhinia acuminata</i>	<i>Polyalthia longifolia</i>	<i>Alstonia scholaris</i>	<i>Neolamarckia cadamba</i>	<i>Plumeria alba</i>
Ba	1.04 ± 0.81	1.06 ± 0.08	1.05 ± 0.18	1.82 ± 0.46	6.03 ± 1.07	1.26 ± 0.01	1.00 ± 0.07	1.44 ± 0.76
CHR	0.26 ± 0.03	0.11 ± 0.06	0.14 ± 0.02	0.26 ± 0.23	0.79 ± 0.38	0.29 ± 0.08	0.10 ± 0.01	0.27 ± 0.001
BbF	2.78 ± 2.00	9.56 ± 1.10	1.54 ± 0.68	4.42 ± 0.17	6.20 ± 1.72	5.45 ± 0.53	1.23 ± 0.46	2.25 ± 1.25
BkF	6.21 ± 1.09	4.78 ± 0.71	2.44 ± 0.60	7.66 ± 0.35	9.84 ± 1.45	8.38 ± 0.66	1.42 ± 0.21	3.07 ± 0.49
BaP	4.35 ± 2.07	53.13 ± 4.28	6.98 ± 3.11	12.99 ± 4.55	15.87 ± 6.54	41.89 ± 0.40	4.74 ± 1.95	9.02 ± 1.56
DB[ah]	2.13 ± 1.69	9.56 ± 4.56	3.84 ± 1.71	9.74 ± 2.22	12.06 ± 3.73	18.01 ± 3.09	2.42 ± 1.05	3.25 ± 1.41
A								
IP	45.59 ± 2.42	14.90 ± 1.88	64.39 ± 1.85	32.59 ± 7.94	29.21 ± 2.71	16.76 ± 1.92	53.56 ± 1.19	56.98 ± 0.57
B[ghi]P	37.64 ± 3.08	6.90 ± 3.44	19.62 ± 2.85	30.52 ± 5.33	20.0 ± 5.08	7.96 ± 5.47	35.53 ± 1.98	23.72 ± 1.94

oxides, sulphur dioxide and ozone) and organic acids) (Latwal et al., 2023; Sharma et al., 2019). Further, pH was also found to be positively influenced by the concentrations of PM ($r = 0.78$, $p < 0.05$) and PAHs ($r = 0.66$, $p < 0.05$), because of its involvement in stress resistance response by increasing the content of AA in tolerant plant types with the increase in pollutants' load (Khanoranga and Khalid, 2019). Among the species considered, *T. divaricata* and *N. oleander* presented highest pH values and the lowest was recorded for *P. longifolia*.

3.4.4. Relative water content (RWC)

Leaf RWC is essentially required for plant photosynthesis, respiration, transpiration, growth, yield, health and tolerance (Malav et al., 2022; Singh et al., 2023). In this study, RWC varied in the range of 65.16–88.93% (Table 3) among the plant types. In view of the responses of plant leaves based on water status to continuous air pollution exposure, RWC displayed a negative relationship with foliar PM load ($r = -0.61$, $p < 0.05$), implying perturbations in plant cell wall permeability, water transportation and balance caused by the accumulation of particulate pollutants or aerosols on leaf canopy with a concomitant reduction in the rate of transpiration owing to clogged stomata (Malav et al., 2022; Zilaie et al., 2023). On the contrary, a weak correlation ($r = 0.21$, $p < 0.05$) was found to exist between RWC and total PAHs. Increased tolerance of plants to atmospheric pollution with high RWC

through the regulation of functional mechanisms driving plant morpho-physiology has been reported in multiple investigations (Karmakar and Padhy, 2019; Kumar et al., 2023). Decline in the rate of carbon assimilation process and reduction in stomatal conductance are the known effects of lower RWC (Lawlor, 2002). In the present work, high values of RWC were seen in the leaves of *N. cadamba*, *A. scholaris*, *C. gigantea* and *P. alba*, while *P. longifolia* showed minimum leaf RWC. Similar observations of dust and heavy metal stress on leaf RWC of various plants from urban terrain were made by Nadgorska-Socha et al. (2017) and Yaghmaei et al. (2022).

3.4.5. Membrane stability index (MSI) and electrolyte leakage (EL): role of proline accumulation

Cellular membranes of plants are highly susceptible to abiotic toxicants which trigger membrane damage, thereby increasing EL and cell secretion as a result of increased membrane permeability (Ma et al., 2019). Recurrent exposure to air pollutants stimulates excessive production of ROS in plant cells, which, in turn, catalyse the conversion of membrane lipids (phospholipids and polyunsaturated fatty acids) into lipid peroxides, causing disintegration and dysfunctioning of cell membranes, and eventually cell necrosis (accidental cell death) (Rangani et al., 2018). Thus, plants manifesting structural and functional integrity of plasma membranes (with high MSI) for cell survival are

Table 3Evaluation of leaf characteristics (as mean \pm SD) of selected plant species as potential biomarkers.

Parameters	Plant species							
	<i>Nerium oleander</i>	<i>Tabernaemontana divaricata</i>	<i>Calotropis gigantea</i>	<i>Bauhinia acuminata</i>	<i>Polyalthia longifolia</i>	<i>Alstonia scholaris</i>	<i>Neolamarckia cadamba</i>	<i>Plumeria alba</i>
Chl a (mg g^{-1} d.w.)	0.57 \pm 0.05	3.62 \pm 0.28	2.93 \pm 0.06	2.02 \pm 0.05	1.80 \pm 0.08	0.98 \pm 0.04	3.43 \pm 0.16	2.84 \pm 0.11
Chl b (mg g^{-1} d.w.)	0.33 \pm 0.07	1.51 \pm 0.06	1.11 \pm 0.09	0.84 \pm 0.05	0.92 \pm 0.04	0.46 \pm 0.05	0.81 \pm 0.04	1.06 \pm 0.08
Chl T (mg g^{-1} d.w.)	0.90 \pm 0.03	5.13 \pm 0.34	4.04 \pm 0.15	2.86 \pm 0.10	2.72 \pm 0.11	1.44 \pm 0.07	4.24 \pm 0.20	3.90 \pm 0.18
Chl a/b	1.73 \pm 0.74	2.39 \pm 0.08	2.64 \pm 0.19	2.40 \pm 0.09	1.96 \pm 0.01	2.13 \pm 0.18	4.23 \pm 0.03	2.68 \pm 0.13
C _x + c (mg g^{-1} d.w.)	0.24 \pm 0.01	1.12 \pm 0.28	0.88 \pm 0.07	0.87 \pm 0.05	1.12 \pm 0.13	0.35 \pm 0.02	1.10 \pm 0.11	0.80 \pm 0.05
AA (mg g^{-1} d.w.)	15.75 \pm 0.44	18.00 \pm 0.27	10.88 \pm 0.26	7.88 \pm 0.18	3.63 \pm 0.08	7.50 \pm 0.18	9.88 \pm 0.08	11.63 \pm 0.09
Leaf extract pH	7.38 \pm 0.05	7.47 \pm 0.04	6.45 \pm 0.04	6.63 \pm 0.07	5.91 \pm 0.06	6.36 \pm 0.05	6.49 \pm 0.06	6.56 \pm 0.08
RWC (%)	76.90 \pm 0.13	70.39 \pm 0.33	84.55 \pm 0.39	78.19 \pm 0.07	65.16 \pm 0.15	85.78 \pm 0.48	88.93 \pm 0.74	81.89 \pm 0.63
MSI (%)	80.52 \pm 2.84	88.69 \pm 4.05	78.01 \pm 4.37	55.27 \pm 6.39	47.59 \pm 6.25	53.90 \pm 3.34	60.79 \pm 3.81	75.44 \pm 4.20
EL (%)	0.98 \pm 0.30	2.31 \pm 0.42	7.29 \pm 0.57	8.93 \pm 1.52	5.21 \pm 0.88	6.10 \pm 0.95	5.60 \pm 0.43	8.26 \pm 0.65
Proline content (mg g^{-1} d.w.)	4.28 \pm 0.59	4.72 \pm 0.18	3.56 \pm 0.73	0.55 \pm 0.13	1.56 \pm 0.49	1.27 \pm 0.37	2.54 \pm 0.66	2.44 \pm 0.58
Leaf carbon content (%)	51.50 \pm 1.24	52.43 \pm 0.95	46.77 \pm 2.45	48.96 \pm 4.54	43.64 \pm 1.24	49.32 \pm 0.89	47.80 \pm 0.23	49.74 \pm 1.29
TSS content (mg g^{-1} d.w.)	15.05 \pm 2.29	24.75 \pm 4.31	10.84 \pm 2.35	9.38 \pm 2.68	5.48 \pm 1.84	4.17 \pm 1.03	7.90 \pm 2.32	12.58 \pm 1.45
Protein content (mg g^{-1} d.w.)	30.72 \pm 3.51	29.75 \pm 2.07	33.42 \pm 3.27	34.81 \pm 2.55	33.37 \pm 4.42	40.09 \pm 3.45	34.86 \pm 4.21	31.46 \pm 2.02
APTI	20.73 \pm 2.07	29.72 \pm 3.15	19.87 \pm 1.58	15.29 \pm 0.46	9.65 \pm 0.89	14.43 \pm 1.20	19.49 \pm 0.48	20.35 \pm 1.99
Total PM load ($\mu\text{g cm}^{-2}$) ^a	1808.64 \pm 46.99	2766.27 \pm 86.79	709.91 \pm 71.34	1697.57 \pm 95.76	1100.44 \pm 94.77	932.61 \pm 89.93	539.32 \pm 101.49	1054.27 \pm 112.85
Total PAHs concentration ($\mu\text{g g}^{-1}$) ^a	286.08 \pm 32.65	393.01 \pm 30.34	267.47 \pm 11.49	177.22 \pm 14.57	159.92 \pm 21.23	256.80 \pm 32.31	301.13 \pm 37.31	342.28 \pm 25.38

^a Though these values are indicated in the body of the manuscript, these are again represented here for the ease of comparative/correlation study.

considered to be pollution tolerant species in biomonitoring (Ahmadi-zadeh et al., 2011). Hence, MSI and EL are better suited as pollution biomarkers for the determination of radical-induced cell membrane damage or injury (Shanazari et al., 2018; Zhang et al., 2022).

In accordance with the results depicted in Table 3, MSI revealed positive correlation with PM ($r = 0.51$, $p < 0.05$) and PAHs ($r = 0.82$, $p < 0.05$), whereas, EL appeared to be negatively correlated with PM ($r = -0.54$, $p < 0.05$) and PAHs ($r = -0.40$, $p < 0.05$). Such outcome is suggestive of the proline-mediated resistance mechanisms of plants for stress management. Proline acts as cytoplasmic osmolyte or osmoprotectant (capable of lowering osmotic potential) and ROS scavenger, which prevents disruption of cell membranes and structural collapse of biomolecules, such as proteins and DNA, promoting stress tolerance in plants through the activation of enzymatic antioxidant system (Hayat et al., 2012; Raza et al., 2023). It also modulates biochemical cascades for stress recovery, improving the performance of plants under polluted atmosphere. These inferences are again endorsed by the positive association between proline content (ref. Table 3) and abiotic stress due to PM ($r = 0.44$, $p < 0.05$) and PAHs ($r = 0.74$, $p < 0.05$). It also played a defensive role in sustaining membrane stability and reducing EL (as confirmed by the positive linear relationship ($r = 0.90$, $p < 0.05$) between MSI and proline and negative correlation, $r = -0.72$, $p < 0.05$, between EL and proline). This study supports the previous findings of Gomes et al. (2010) and Sameena and Puthur (2021). It has been mostly seen that EL is predominantly accompanied by the efflux of potassium ions (K^+) from plant cells. Therefore, it should be emphasized that tolerant species impede the excessive release of K^+ (i.e. avoid EL) and uphold potassium homeostasis regulating plant cell physiology (Shabala and Cuin, 2008). *N. oleander* and *T. divaricata* showed highest percentages (80.52 and 88.69% respectively) of MSI and maximum proline contents (4.28 and 4.72 mg g^{-1} respectively) with minimum EL (0.98 and 2.31% respectively). *C. gigantea*, *N. cadamba* and *P. alba*, though exhibiting high EL % (5.60–8.26), presented higher values of MSI (60.79–78.01%) because of substantial proline content (2.44–3.56 mg

g^{-1}) that may be considered to be responsible for initiation of the stress recovery process. However, minimum concentrations (0.55–1.56 mg g^{-1}) of proline as recorded in *B. acuminata*, *P. longifolia* and *A. scholaris* had initiated appreciable ion leakages (5.21–8.93%) in the foliage rendering the MSI values (47.59–55.27%) to be lowest, proving the sensitive nature of the said plants.

3.4.6. Leaf carbon content: carbon allocation in stress tolerance

Plants having sessile nature are constantly exposed to environmental changes unfavourable for their survival and growth. Therefore, utilization of all the viable resources at plants' disposal would be the response of plants towards ensuring sustained growth and yield as well as combating pollution load with negation of ensuing stress injury. Among all the resources, carbon allocation may be termed as one of the most important processes of plants' defense mechanism (Hartmann and Trumbore, 2016; Hartmann et al., 2020; Xia et al., 2017). PM-induced stomatal blockage lowers the CO_2 uptake by plants and hampers photosynthesis (Saxena and Kulshrestha, 2016), thereby prompting reallocation of carbon—need throughout the plant body (Kobe et al., 2010). As a result, carbon content of plant leaves makes it an effective biomarker of plant health against pollution. Differences in the leaf carbon contents of native species are demonstrated in Table 3. Carbon content of 43.64–52.43% implied increased carbon allocation and synthesis of carbon compounds in the leaf tissues for stress resilience. Occurrences of positive correlations of carbon with PM ($r = 0.66$, $p < 0.05$) and PAHs ($r = 0.72$, $p < 0.05$) also prove the above contention. Foliar carbon contents were found to be highest in *T. divaricata* and *N. oleander* and lowest in *P. longifolia* (Table 3). Comparable carbon percentages (42.4%) in the overground tissues of vegetation of arid ecosystem were also noticed by Juan et al. (2014). Drake et al. (2019) and Xia et al. (2017) observed enhanced carbon distribution in the aboveground parts of the plants (leaf, wood, etc.) in comparison to belowground part for physiological processes (i.e. respiration, growth, etc.) in presence of environmental stressors such as drought, warming, high water and low

light conditions. Paull et al. (2021) investigated carbon content of green wall species subjected to atmospheric pollution and inferred it to be a health response mediated by plants.

3.4.7. Total soluble sugar (TSS) content

TSS is usually regarded as another type of osmo-regulator (other than proline) which strengthens cell stability and turgor in plants and also triggers ROS defense machinery, protecting cellular components and controlling signaling pathways during stress (Rai, 2016). Plant sensitivity is associated with low TSS owing to the collateral effects of relatively less pollutant bioaccumulation capacity and structural impairment of leaf chlorophyll (Banerjee et al., 2021). Synergistic interactions of TSS with antioxidants at tissue and cellular levels impart stress tolerance to plants (Bolouri-Moghaddam et al., 2010). The current study also supports the above inferences (based on the results given in Table 3) as revealed by the positive correlations of TSS content with PM ($r = 0.82$, $p < 0.05$), PAHs ($r = 0.74$, $p < 0.05$), proline ($r = 0.80$, $p < 0.05$), AA ($r = 0.91$, $p < 0.05$), $C_x + c$ ($r = 0.15$, $p < 0.05$) and Chl_T ($r = 0.46$, $p < 0.05$). This can be comprehended from the above correlations that the increase in pollution stress favours increased bio-synthesis and accumulation of TSS which acts in conjunction with the enhanced levels of proline and AA, maintaining higher levels of Chl_T to counterbalance the toxicity of pollutants for sustenance and growth of plants. However, it was noted that the $C_x + c$ have minimal direct impact on TSS which was, contrarily, found to have pronounced effect on leaf carbon content ($r = 0.72$, $p < 0.05$) as TSS might be considered as a primary carbon source for energy generation. The TSS accumulation was highest in *T. divaricata* and *N. oleander* with leaf concentrations of 24.75 and 15.05 mg g⁻¹ respectively and lowest in *P. longifolia* (5.48 mg g⁻¹) and *A. scholaris* (4.17 mg g⁻¹). Jeddi et al. (2021) and Kamble et al. (2021) also detected high concentrations of TSS in the plant leaves of polluted sites, suggesting the multifaceted roles of soluble sugars.

3.4.8. Protein content

Besides being principal building blocks for different aspects of plant growth such as structural growth with biomass change, expansive growth, cell production and proliferation, etc., protein molecules also govern the cellular stress responses to environmental gradients (Qazi et al., 2019). Pollution stress-mediated toxicity may act as an inducing factor for rise or decline of protein content in plant types based on their intrinsic capabilities of enduring abiotic stress (Rai, 2016). A declining trend in protein concentration (ref. Table 3) of plant leaves in response to stress was achieved in the present investigation which was affirmed by the inverse relationship of protein with PM ($r = -0.56$, $p < 0.05$), PAHs ($r = -0.46$, $p < 0.05$) and proline ($r = -0.71$, $p < 0.05$). The catalytic presence of pollutants might be deemed to be the inhibitor of *de novo* protein synthesis and also prime mover behind the proteolytic cleavage of peptide bonds degenerating protein structures into minuscule amino acids, thereby enhancing protein reduction (Iqbal et al., 2000). Protein contents of *T. divaricata* (29.75 mg g⁻¹) and *N. oleander* (30.72 mg g⁻¹) were found to be more affected by air pollutants. Likewise, decreased levels of protein content were documented for *F. benghalensis* and *T. arjuna* (sampled from industrial regions) by Banerjee et al. (2022) as well as for *D. alba* and *R. communis* growing along the congested roads with dense traffic by Khalid et al. (2019).

3.4.9. Air pollution induced stress tolerance of plants and considerations for green belting

Studies have indicated that the plants' competences to respond to external stress signals vary in consonance with their biochemical, physiological and morpho-anatomical characteristics for a clean environment of the biosphere, maintaining biogeochemical cycle with ecological balance. From this perspective, plants are explored as important tools in environmental bioindication and biomonitoring depending on their pollution sensitive or tolerant nature (Achakzai et al., 2017). One way of expressing plants' ability for the

above-mentioned purposes is through assessment of APTI which involves Chl_T, AA, leaf pH and RWC for its evaluation. The APTI values, shown in Table 3, reflected *N. oleander*, *T. divaricata*, *C. gigantea*, *N. cadamba* and *P. alba* as tolerant species (APTI: 19.49–29.72, i.e. >17), *B. acuminata* and *A. scholaris* as intermediately tolerant (APTI: 15.29 and 14.43 respectively, i.e. lying between 10 and 16) and *P. longifolia* as a sensitive one (APTI: 9.65, i.e. <10). Moreover, APTI varied positively with PM ($r = 0.58$, $p < 0.05$) and PAHs ($r = 0.90$, $p < 0.05$), suggesting a direct relationship with high pollution levels. Strong positive influences of AA ($r = 0.94$, $p < 0.05$), pH ($r = 0.84$, $p < 0.05$) and Chl_T ($r = 0.55$, $p < 0.05$) on APTI are also considerable pertaining to the structural and functional stability of the plants against stress-causing factors. Weak correlation between RWC and APTI ($r = 0.06$, $p < 0.05$) defined low dependence of APTI on RWC for all the investigated species. Thus, high APTI values signify enhanced competitive abilities of stress tolerant plants for biomonitoring of urban pollution through adaptive mechanisms (Kamble et al., 2021).

Being pollution indicators, plants change their responses with varying degrees of anthropogenic contamination. Hence, strategic selection of tolerant plants for green spaces is obligatory in order to ensure urban sustainability through the obtainment of maximum area-cover served by the green zone. Concerning biomonitoring, primary selection of plants is usually based on APTI analysis, but the grade of their performance should be critically judged through the application of API which also includes the impact of APTI along with other plant traits (as discussed in section 2.5) (Bala et al., 2022). Performance factor assessment with respect to plant species gradation and API has been represented in Table 4. *N. cadamba* (93.75%), *N. oleander* (81.25%) and *P. alba* (81.25%) have highest API score and are ranked as highly competent species with best and excellent performance. *T. divaricata*, *C. gigantea* and *A. scholaris* are also screened as very good and good performers (as seen from Table 4), although *A. scholaris* displayed intermediate tolerance on APTI scale. In addition, *B. acuminata*, though lying in the poor category as per API grade, showed better performance in PM capture because of the leaf shape with the presence of specialized appendages or trichomes on leaf surfaces (ref. section 3.1). In a recent study, Patel et al. (2023) proposed that the plants scoring a percentage value of less than 50% need not be considered for planting designs in urban canyons. However, in spite of being sensitive from APTI screening, *P. longifolia* proved to be a moderate performer on the basis of API gradation. This has coherence with the results showing accumulation and encapsulation of particulates due to their distinctive macro- and microscale properties with prominent topographical structures on the surfaces of the leaves (as elaborated in section 3.1). Many studies offered comprehensive descriptions on the key aspects of APTI and API with major thrust on the broader outline of green belting using native flora (Goswami et al., 2022; Patel et al., 2023).

In this context, it may be argued that the plants' tolerance or adaptability does not only depend on APTI or API scale, but there are several other biochemical, physiological, morphological, environmental and topographical variables contributing to their pollution tolerance capacities (Banerjee et al., 2022). In line with the above statement, the present study focused on the multiparametric analysis highlighting the influences of pollutants (PM and PAHs), foliar morphology, leaf wax, SLA, Chl a/b, $C_x + c$, MSI, EL, proline, leaf carbon, TSS and protein apart from APTI/API and as such correlation analysis substantiated the strength of association between leaf traits and airborne pollutants. Even though RWC and protein revealed negative correlations with pollutants, Chl a/b, $C_x + c$, AA, leaf pH, MSI, EL, proline, leaf carbon and TSS had beneficial impacts on plant responses. Variability assessment of more number of biomarkers would throw open the options of choosing the plant types from a vast reserve of vegetation depending on their enhanced probability of positive correlation with air pollution, rendering the vista of green belting wide open with the inclusions of species-diversified plant communities. However, APTI and API may serve the purpose of quick selection of the tolerant species.

Table 4

Anticipated Performance Index (API) of selected plant species.

Plant species	APTI	Plant habit	Canopy structure	Type of plant	Laminar structure			Economic value	Grade allotted			Assessment Category (AC)
					Size	Texture	Hardiness		Total plus (+)	% score	API value/ Grade	
<i>Nerium oleander</i>	+++++	+	+	+	++	+	+	+	13	81.25	6	Excellent
<i>Tabernaemontana divaricata</i>	+++++	+	+	+	+	+	-	++	12	75	5	Very good
<i>Calotropis gigantea</i>	++++	+	+	+	++	+	-	++	12	75	5	Very Good
<i>Bauhinia acuminata</i>	+++	-	+	-	+	+	+	+	8	50	2	Poor
<i>Polyalthia longifolia</i>	+	++	+	+	+	+	+	+	9	56.25	3	Moderate
<i>Alstonia scholaris</i>	++	++	++	+	++	+	+	-	11	68.75	4	Good
<i>Neolamarckia cadamba</i>	++++	++	++	+	++	+	+	++	15	93.75	7	Best
<i>Plumeria alba</i>	+++++	+	+	-	++	+	+	++	13	81.25	6	Excellent

Maximum grade of 16 can be scored by any plant. % Score (≤ 30) = Grade 0 (AC: Not recommended); % Score (31–40) = Grade 1 (AC: Very poor); % Score (41–50) = Grade 2 (AC: Poor); % Score (51–60) = Grade 3 (AC: Moderate); % Score (61–70) = Grade 4 (AC: Good); % Score (71–80) = Grade 5 (AC: Very good); % Score (81–90) = Grade 6 (AC: Excellent); % Score (91–100) = Grade 7 (AC: Best) (Prajapati and Tripathi, 2008b; Pathak et al., 2011; Pandey et al., 2015b; Kaur and Nagpal, 2017).

Regarding green belt formation considering building geometry and plant height combination, Liu et al. (2023) suggested that relatively longer building length with respect to width and alternate tree and hedge arrangement would prove more beneficial in reducing the effect of particles in urban sprawl. This may also be applicable with double rows of tree arrangement. Wu et al. (2021) observed that the mixed designs with small shrubs and arbour–shrub combination at maximum concentration distance would substantially lower the exposure risks to pedestrians and pollutant concentrations in horizontal dispersion. In case of vertical dispersion, the authors found that the shrubs served the purpose of inhibition of pollutant diffusion through wind flow, resulting in faster deposition of PM within a height of 2–4 m. Conversely, Li et al. (2016) inferred that the low height of shrub mediated increase in the vertical movement and transportation of PM, thereby reducing ambient concentrations. Based on the above facts, it could be opined that after species selection, the following factors for planting arrangement should be considered in order to make the design effective and more conducive for maximum removal of pollutants — urban morphology/design, area under study including topography, vegetation composition and distribution, vegetation density index and coverage ratio, plant height, crown diameter, soil and water quality, aspect ratio (building width:height) and meteorological factors. Therefore, all the studied species may be surmised to be included in urban road green belt construction for alleviating somehow or other near roadway pollutant concentrations.

4. Conclusion

The present study has focused on the selection of local but abundant terrestrial plant species as air pollution biomonitoring of tolerant types under pollution load based on their PM and PAHs retention abilities. Deposition of surface PM ($493\text{--}2680 \mu\text{g cm}^{-2}$) and wax PM ($5.30\text{--}25.82 \mu\text{g cm}^{-2}$) of size $10\text{--}100 \mu\text{m}$ was prominent in the leaves of all the species showing maximum surface accumulation of PM of all particle sizes. *T. divaricata*, *N. oleander*, *B. acuminata*, *P. longifolia* and *P. alba* were efficient PM retainers. The particle accumulation by plant foliage was found to have definite correlations with leaf waxes, shape and microstructural variability. PAHs concentrations were detected in the range of $159.92\text{--}393.01 \mu\text{g g}^{-1}$ in the plant leaves. In, *N. oleander*, *T. divaricata*, *C. gigantea* and *N. cadamba*, HMW PAHs (53–62%) were predominant, while composition profiles of *B. acuminata*, *P. longifolia*, *A. scholaris* and *P. alba* showed the prevalence of LMW PAHs (51–57%). TI values of more than 4 implied the presence of combustion emitted PAHs, more specifically those released from traffic emissions. The toxicological risk analyses revealed carcinogenic and mutagenic hazards from mainly HMW PAHs (>90% contribution). Parameters such as Chl a/b, C_{X+C}, AA, leaf pH, proline, leaf carbon and TSS were examined as

controlling variables by correlation analysis, imparting tolerance to the plants through maintenance of Chl_T, membrane stability (viz. MSI) and ion leakage (viz. EL), under high air pollution stress severity. Abiotic stressors also triggered reduction in leaf RWC and protein content as stress symptoms.

T. divaricata and *N. oleander* are highly recommendable for green belting because of their specific leaf traits, APTI and API values along with PM and PAHs capturing capabilities. Also, *N. cadamba*, *C. gigantea* and *P. alba* with high APTI and API are suitable options for air pollution mitigation, *P. alba* being superior to the first two species in PM capturing and PAHs accumulation. *B. acuminata* and *P. longifolia* may be utilized in some specific areas with dust-laden atmosphere because of their effectiveness in high PM removal with moderate potential of PAHs biofiltration. On the other hand, PAHs filtering behaviour of *A. scholaris* with average PM retention ability makes it an obvious choice for designing urban green spaces in densely populated areas. From the above, it can be recommended that the selected shrubs and trees of native origin and fast-growing nature should be planted in combination in a staggered formation to prevent wind funnelling with due considerations to their orientation relative to the locations of industrial and housing belts with road network. The available inter-spaces between trees should also be covered with meadows (particularly dominated by grasses, herbs or non-woody plants) or hedges to form an effective barrier by lessening the gaps. Future experimentations on lower plants (bryophytes and lichens) should be orchestrated for their structures and high particle capturing capacities for improved biomonitoring of ambient air with variable pollution intensities.

Contribution

RD planned and supervised the whole work and reviewed the manuscript.

Contribution

SM had done the experiments and had written the manuscript.

Contribution

PD had checked and reviewed the manuscript.

CRediT authorship contribution statement

Shritama Mukhopadhyay: Writing – original draft, Data curation. **Ratna Dutta:** Writing – review & editing, Supervision, Conceptualization. **Papita Das:** Writing – review & editing.

Declaration of competing interest

The authors declare that they have no known competing financial interests or personal relationships that could have appeared to influence the work reported in this paper.

Data availability

No data was used for the research described in the article.

Acknowledgement

The authors would like to acknowledge the support received from the Department of Chemical Engineering, Jadavpur University, Kolkata, India, in terms of resources and facilities towards achieving successful results. The authors are sincerely thankful to the Department of Metallurgy and Materials Engineering, Indian Institute of Engineering Science and Technology (IEST), Shibpur, Howrah, West Bengal, India, for SEM analysis. The authors are also grateful to the State Government Fellowship Scheme of Jadavpur University for providing Senior Research Fellowship to SM.

Appendix A. Supplementary data

Supplementary data to this article can be found online at <https://doi.org/10.1016/j.jenvman.2024.120524>.

References

- Abeyasinghe, P.D., Scharaschkin, T., 2022. Comparative anatomy of two forms of Sri Lankan *Catotropis gigantea* (L.) R. Br. (Family Apocynaceae s.l. – Subfamily Asclepiadoideae) -Taxonomic implications. Ceylon J. Sci. 51, 307–318. <https://cjs.sljol.info/articles/10.4038/cjs.v51i3.8038>.
- Achakzai, K., Khalid, S., Adrees, M., Bibi, A., Ali, S., Nawaz, R., Rizwan, M., 2017. Air pollution tolerance index of plants around brick kilns in Rawalpindi, Pakistan. J. Environ. Manag. 190, 252–258. <https://doi.org/10.1016/j.jenvman.2016.12.072>.
- Adhikari, S., Siebert, S.J., Jordaan, A., 2021. Evidence of chromium dust pollution on the leaves of food and medicinal plants from mining areas of Sekhukhuneland, South Africa. South Afr. J. Bot. 143, 226–237. <https://doi.org/10.1016/j.sajb.2021.08.007>.
- Ahmadiزاده, M., نوری, A., شاهبازی, H., حبیبپور, M., 2011. Effects of drought stress on some agronomic and morphological traits of durum wheat (*Triticum durum* Desf.) landraces under greenhouse condition. Afr. J. Biotechnol. 10, 14097–14107. <https://doi.org/10.5897/AJB11.2322>.
- Amabde, B., Sethi, S.S., Kurwadkar, S., Mishra, P., Tripathee, L., 2022. Accumulation of polycyclic aromatic hydrocarbons (PAHs) in surface sediment residues of Mahanadi River Estuary: abundance, source, and risk assessment. Mar. Pollut. Bull. 183, 114073 <https://doi.org/10.1016/j.marpolbul.2022.114073>.
- Anand, P., Mina, U., Khare, M., Kumar, P., Kota, S.H., 2022. Air pollution and plant health response-current status and future directions. Atmos. Pollut. Res. 13, 101508 <https://doi.org/10.1016/j.apr.2022.101508>.
- Bala, N., Pakade, Y.B., Katnoria, J.K., 2022. Assessment of air pollution tolerance index and anticipated performance index of a few local plant species available at the roadside for mitigation of air pollution and green belt development. Air Qual. Atmos. Health 15, 2269–2281. <https://doi.org/10.1007/s11869-022-01251-7>.
- Banerjee, S., Banerjee, A., Palit, D., 2022. Morphological and biochemical study of plant species—a quick tool for assessing the impact of air pollution. J. Clean. Prod. 339, 130647 <https://doi.org/10.1016/j.jclepro.2022.130647>.
- Banerjee, S., Banerjee, A., Palit, D., Roy, R., 2019. Assessment of vegetation under air pollution stress in urban industrial area for greenbelt development. Int. J. Environ. Sci. Technol. 16, 5857–5870. <https://doi.org/10.1007/s13762-018-1963-9>.
- Banerjee, S., Palit, D., Banerjee, A., 2021. Variation of tree biochemical and physiological characters under different air pollution stresses. Environ. Sci. Pollut. Res. 28, 17960–17980. <https://doi.org/10.1007/s11356-020-11674-3>.
- Bates, L.S., Waldren, R.P., Teare, I.D., 1973. Rapid determination of free proline for water-stress studies. Plant Soil 39, 205–207. <https://www.jstor.org/stable/42932378>.
- Baxter, X.C., Darvell, L.I., Jones, J.M., Barraclough, T., Yates, N.E., Shield, I., 2014. Miscanthus combustion properties and variations with Miscanthus agronomy. Fuel 117, 851–869. <https://doi.org/10.1016/j.fuel.2013.09.003>.
- Blaszczyk, E., Rogula-Kozlowska, W., Klejnowski, K., Fulara, I., Mielzynska-Svach, D., 2017. Polycyclic aromatic hydrocarbons bound to outdoor and indoor airborne particles (PM_{2.5}) and their mutagenicity and carcinogenicity in Silesian kindergartens, Poland. Air Qual. Atmos. Health 10, 389–400. <https://doi.org/10.1007/s11869-016-0457-5>.
- Bolouri-Moghaddam, M.R., Roy, K.L., Xiang, L., Rolland, F., Van den Ende, W., 2010. Sugar signalling and antioxidant network connections in plant cells. FEBS J. 277, 2022–2037. <https://doi.org/10.1111/j.1742-4658.2010.07633.x>.
- Borgulat, J., Borgulat, A., 2023. Biomonitoring of atmospheric PAHs using fir and spruce needles in forests in the vicinity of mountain villages. Environ. Pollut. 330, 121814 <https://doi.org/10.1016/j.envpol.2023.121814>.
- Bradford, M.M., 1976. A rapid and sensitive method for the quantitation of micro-gram quantities of protein utilizing the principle of protein-dye binding. Anal. Biochem. 72, 248–254. [https://doi.org/10.1016/0003-2697\(76\)90527-3](https://doi.org/10.1016/0003-2697(76)90527-3).
- Brantley, H.L., Hagler, G.S.W., Deshmukh, P.J., Baldauf, R.W., 2014. Field assessment of the effects of roadside vegetation on near-road black carbon and particulate matter. Sci. Total Environ. 468, 120–129. <https://doi.org/10.1016/j.scitotenv.2013.08.001>.
- Cai, M., Xin, Z., Yu, X., 2017. Spatio-temporal variations in PM leaf deposition: a metaanalysis. Environ. Pollut. 231, 207–218. <https://doi.org/10.1016/j.envpol.2017.07.105>.
- Chowdhury, A.S., Uddin, M.J., Baul, T.K., Akhter, J., Nandi, R., Karmakar, S., Nath, T.K., 2022. Quantifying the potential contribution of urban trees to particulate matters removal: a study in Chattogram city, Bangladesh. J. Clean. Prod. 380, 135015 <https://doi.org/10.1016/j.jclepro.2022.135015>.
- Corada, K., Woodward, H., Alaraj, H., Collins, C.M., de Nazelle, A., 2021. A systematic review of the leaf traits considered to contribute to removal of airborne particulate matter pollution in urban areas. Environ. Pollut. 269, 116104 <https://doi.org/10.1016/j.envpol.2020.116104>.
- Delgado-Saborit, J.M., Stark, C., Harrison, R.M., 2011. Carcinogenic potential, levels and sources of polycyclic aromatic hydrocarbon mixtures in indoor and outdoor environments and their implications for air quality standards. Environ. Int. 37, 383–392. <https://doi.org/10.1016/j.envint.2010.10.011>.
- De Nicola, F., Grana, E.C., Aboal, J.R., Carballoira, A., Fernandez, J.A., Mahia, P.L., Rodriguez, D.P., Lorenzo, S.M., 2016. PAH detection in *Quercus robur* leaves and *Pinus pinaster* needles: a fast method for biomonitoring purpose. Talanta 153, 130–137. <https://doi.org/10.1016/j.talanta.2016.01.067>.
- De Nicola, F., Grana, E.C., Mahia, P.L., Lorenzo, S.M., Rodriguez, D.P., Retuerto, R., Carballoira, A., Aboal, J.R., Fernandez, J.A., 2017. Evergreen or deciduous trees for capturing PAHs from ambient air? A case study. Environ. Pollut. 221, 276–284. <https://doi.org/10.1016/j.envpol.2016.11.074>.
- Desalme, D., Binet, P., Chiapuiso, G., 2013. Challenges in tracing the fate and effects of atmospheric polycyclic aromatic hydrocarbon deposition in vascular plants. Environ. Sci. Technol. 47, 3967–3981. <https://doi.org/10.1021/es304964b>.
- Drake, J.E., Tjoelker, M.G., Aspinwall, M.J., Reich, P.B., Pfautsch, S., Barton, C.V.M., 2019. The partitioning of gross primary production for young *Eucalyptus tereticornis* trees under experimental warming and altered water availability. New Phytol. 222, 1298–1312. <https://doi.org/10.1111/nph.15629>.
- Duarte-Almeida, J.M., Clemente, M.S., Arruda, R.C.O., Vaz, A.M.S.F., Salatino, A., 2015. Glands on the foliar surfaces of tribe Cercideae (Caesapiodiaceae, Leguminosae): distribution and taxonomic significance. An. Acad. Bras. Cienc. 87, 787–796. <https://doi.org/10.1590/0001-3765201520140151>.
- Durant, J., Busby, W., Lafleur, A., Penman, B., Crespi, C., 1996. Human cell mutagenicity of oxygenated, nitrated and unsubstituted polycyclic aromatic hydrocarbons associated with urban aerosols. Mutat. Res. Genet. Toxicol. 371, 123–157. [https://doi.org/10.1016/S0165-1218\(96\)90103-2](https://doi.org/10.1016/S0165-1218(96)90103-2).
- Dzierzanowski, K., Popek, R., Gawronski, H., Saebo, A., Gawronski, S.W., 2011. Deposition of particulate matter of different size fractions on leaf surfaces and in waxes of urban forest species. Int. J. Phytoremediation 13, 1037–1046. <https://doi.org/10.1080/15226514.2011.552929>.
- El-Khatib, A.A., El-Rahman, A.M.A., El-Sheikh, O.M., 2012. Biomagnetic monitoring of air pollution using dust particles of urban tree leaves at upper Egypt. Assiut Univ. J. Bot. 41, 111–130.
- Enete, I.C., Chukwudelu, V.U., Okolie, A.O., 2013. Evaluation of air pollution tolerance index of plants and ornamental shrubs in Enugu City: implications for urban heat island effect. World Environ. 3, 108–115.
- Escobedo, F.J., Wagner, J.E., Nowak, D.J., De la Maza, C.L., Rodriguez, M., Crane, D.E., 2008. Analyzing the cost effectiveness of Santiago, Chile's policy of using urban forests to improve air quality. J. Environ. Manag. 86, 148–157. <https://doi.org/10.1016/j.jenvman.2006.11.029>.
- Foan, L., Simon, V., 2012. Optimization of pressurized liquid extraction using a multivariate chemometric approach and comparison of solid-phase extraction cleanup steps for the determination of polycyclic aromatic hydrocarbons in mosses. J. Chromatogr. A 1256, 22–31. <https://doi.org/10.1016/j.chroma.2012.07.065>.
- Fred-Ahmadu, O.H., Benson, N.U., 2019. Polycyclic aromatic hydrocarbons (PAHs) occurrence and toxicity in *Camellia sinensis* and Herbal Tea. Polycycl. Aromat. Comp. 39, 383–393. <https://doi.org/10.1080/10406638.2017.1335216>.
- Frei, M., Wissuwa, M., Pariasca-Tanaka, J., Chen, C.P., Sudekum, K.H., Kohno, Y., 2012. Leaf ascorbic acid level — is it really important for ozone tolerance in rice? Plant Physiol. Biochem. 59, 63–70. <https://doi.org/10.1016/j.plaphy.2012.02.015>.
- Gemba, K., 2007. Shape Effects on Drag. Department of Aerospace Engineering, California State University. Accessed online on 17-04-2023). <http://gemba.org/wp-content/uploads/2015/11/MAE440Exp01.pdf>.
- Gerdol, R., Bragazza, L., Marchesini, R., Medici, A., Pedrini, P., Benedetti, S., Bovolenta, A., Coppi, S., 2002. Use of moss (*Tortula muralis* Hedw.) for monitoring organic and inorganic air pollution in urban and rural sites in northern Italy. Atmos. Environ. 36, 4069–4075. [https://doi.org/10.1016/S1352-2310\(02\)00298-4](https://doi.org/10.1016/S1352-2310(02)00298-4).
- Ghafari, S., Kaviani, B., Sedaghathoor, S., Allahyari, M.S., 2020. Ecological potentials of trees, shrubs and hedge species for urban green spaces by multi criteria decision making. Urban For. Urban Green. 55, 126824 <https://doi.org/10.1016/j.ufug.2020.126824>.

- Gillies, J.A., Nickling, W.G., King, J., 2002. Drag coefficient and plant form response to wind speed in three plant species: burning bush (*Euonymus alatus*), Colorado Blue Spruce (*Picea pungens glauca*), and Fountain Grass (*Pennisetum setaceum*). *J. Geophys. Res. Atmos.* 107, 1–15. <https://doi.org/10.1029/2001JD001259>.
- Gomes, F.P., Oliva, M.A., Mielke, M.S., Almeida, A.A.F., Aquino, L.A., 2010. Osmotic adjustment, proline accumulation and cell membrane stability in leaves of *Cocos nucifera* submitted to drought stress. *Sci. Hortic.* 126, 379–384. <https://doi.org/10.1016/j.scienta.2010.07.036>.
- Goswami, M., Kumar, V., Kumar, P., Singh, N., 2022. Prediction models for evaluating the impacts of ambient air pollutants on the biochemical response of selected tree species of Haridwar, India. *Environ. Monit. Assess.* 194, 1–16. <https://doi.org/10.1007/s10661-022-10384-2>.
- Goswami, M., Kumar, V., Singh, N., Kumar, P., 2023. A biochemical and morphological study with multiple linear regression modeling-based impact prediction of ambient air pollutants on some native tree species of Haldwani City of Kumaun Himalaya, Uttarakhand, India. *Environ. Sci. Pollut. Res.* 30, 74900–74915. <https://doi.org/10.1007/s11356-023-27563-4>.
- Govindaraju, M., Ganeshkumar, R.S., Muthukumaran, V.R., Visvanathan, P., 2012. Identification and evaluation of air-pollution tolerant plants around lignite-based thermal power station for greenbelt development. *Environ. Sci. Pollut. Res.* 19, 1210–1223. <https://doi.org/10.1007/s11356-011-0637-7>.
- Hajizadeh, Y., Mokhtari, M., Faraji, M., Abdolahnejad, A., Mohammadi, A., 2019. Biomonitoring of airborne metals using tree leaves: protocol for biomonitor selection and spatial trend. *MethodsX* 6, 1694–1700. <https://doi.org/10.1016/j.mex.2019.07.019>.
- Han, Y., Lee, J., Haiping, G., Kim, K.H., Wanxi, P., Bhardwaj, N., Oh, J.M., Brown, R.J.C., 2022. Plant-based remediation of air pollution: a review. *J. Environ. Manag.* 301, 113860. <https://doi.org/10.1016/j.jenvman.2021.113860>.
- Hartmann, H., Bahn, M., Carbone, M., Richardson, A.D., 2020. Plant carbon allocation in a changing world – challenges and progress: introduction to a Virtual Issue on carbon allocation. *New Phytol.* 227, 981–988. <https://doi.org/10.1111/nph.16757>.
- Hartmann, H., Trumbore, S., 2016. Understanding the roles of nonstructural carbohydrates in forest trees – from what we can measure to what we want to know. *New Phytol.* 211, 386–403. <https://doi.org/10.1111/nph.13955>.
- Hayat, S., Hayat, Q., Alyemeni, M.N., Wani, A.S., Pichtel, J., Ahmad, A., 2012. Role of proline under changing environments. *Plant Signal. Behav.* 7, 1456–1466. <https://timesofindia.indiatimes.com/city/kolkata/breathing-citys-toxic-air-is-like-smoking-doctors/articleshow/63423970.cms>. (Accessed 2 February 2024).
- Huang, C.W., Lin, M.Y., Khlystov, A., Katul, G., 2013. The effects of leaf area density variation on the particle collection efficiency in the size range of ultrafine particles (UFP). *Environ. Sci. Technol.* 47, 11607–11615. <https://doi.org/10.1021/es4013849>.
- Ihunwo, O.C., Ibezim-Ezeani, M.U., DelValls, T.A., 2021. Human health and ecological risk of polycyclic aromatic hydrocarbons (PAHs) in sediment of Woji creek in the Niger Delta region of Nigeria. *Mar. Pollut. Bull.* 162, 111903. <https://doi.org/10.1016/j.marpolbul.2020.11190>.
- Iqbal, M., Srivastava, P.S., Siddiqi, T.O., 2000. Anthropogenic stresses in the environment and their consequences. In: Iqbal, M., et al. (Eds.), *Environmental Hazards, Plants and People*. CBS Publishers, New Delhi, pp. 1–40.
- Jamil, S., Abhilash, P.C., Singh, A., Singh, N., Behl, H.M., 2009. Fly ash trapping and metal accumulating capacity of plants: Implication for green belt around thermal power plants. *Landsc. Urban Plann.* 92, 136–147. <https://doi.org/10.1016/j.landurbplan.2009.04.002>.
- Janhall, S., 2015. Review on urban vegetation and particle air pollution — deposition and dispersion. *Atmos. Environ.* 105, 130–137. <https://doi.org/10.1016/j.atmosenv.2015.01.052>.
- Jeddi, K., Siddique, K.H.M., Chaieb, M., Hessini, K., 2021. Physiological and biochemical responses of *Lawsonia inermis* L. to heavy metal pollution in arid environments. *South Afr. J. Bot.* 143, 7–16. <https://doi.org/10.1016/j.sajb.2021.07.015>.
- Jia, J., Bi, C., Zhang, J., Chen, Z., 2019. Atmospheric deposition and vegetable uptake of polycyclic aromatic hydrocarbons (PAHs) based on experimental and computational simulations. *Atmos. Environ.* 204, 135–141. <https://doi.org/10.1016/j.atmosenv.2019.02.030>.
- Juan, Z., Xiu-jun, W., Jia-ping, W., Wei-xia, W., 2014. Carbon and nitrogen contents in typical plants and soil profiles in Yanqi Basin of Northwest China. *J. Integr. Agric.* 13, 648–656. [https://doi.org/10.1016/S2095-3119\(13\)60723-6](https://doi.org/10.1016/S2095-3119(13)60723-6).
- Kacharava, N., Chanishvili, S., Badridze, G., Chkhubianishvili, E., Janukashvili, N., 2009. Effect of seed irradiation on the content of antioxidants in leaves of Kidney bean, Cabbage and Beet cultivars. *Aust. J. Crop. Sci.* 3, 137–145.
- Kamble, P., Bodhaney, P.S., Beig, G., Awale, M., Mukkannavar, U., Mane, A.V., Mujumdar, M., Kuchekar, S.R., Patil, V.N., 2021. Impact of transport sector emissions on biochemical characteristics of plants and mitigation strategy in Pune, India. *Environ. Chall.* 4, 100081. <https://doi.org/10.1016/j.envc.2021.100081>.
- Karmakar, D., Padhy, P.K., 2019. Air pollution tolerance, anticipated performance, and metal accumulation indices of plant species for greenbelt development in urban industrial area. *Chemosphere* 237, 124522. <https://doi.org/10.1016/j.chemosphere.2019.124522>.
- Kaur, M., Nagpal, A.K., 2017. Evaluation of air pollution tolerance index and anticipated performance index of plants and their application in development of green space along the urban areas. *Environ. Sci. Pollut. Res.* 24, 18881–18895. <https://doi.org/10.1007/s11356-017-9500-9>.
- Kaur, R., Pandey, P., 2021. Air pollution, climate change, and human health in Indian cities: a brief review. *Front. Sustain. Cities* 3, 1–18. <https://doi.org/10.3389/frsc.2021.705131>.
- Khalid, N., Masood, A., Noman, A., Aqeel, M., Qasim, M., 2019. Study of the responses of two biomonitor plant species (*Datura alba* & *Ricinus communis*) to roadside air pollution. *Chemosphere* 235, 832–841. <https://doi.org/10.1016/j.chemosphere.2019.06.143>.
- Khanoranga, Khalid, S., 2019. Phytomonitoring of air pollution around brick kilns in Balochistan province Pakistan through air pollution index and metal accumulation index. *J. Clean. Prod.* 229, 727–738. <https://doi.org/10.1016/j.jclepro.2019.05.050>.
- Kobe, R.K., Iyer, M., Walters, M.B., 2010. Optimal partitioning theory revisited: nonstructural carbohydrates dominate root mass responses to nitrogen. *Ecology* 91, 166–179. <https://doi.org/10.1890/09-0027.1>.
- Konczak, B., Cempa, M., Pierzchala, L., Deska, M., 2021. Assessment of the ability of roadside vegetation to remove particulate matter from the urban air. *Environ. Pollut.* 268, 115465. <https://doi.org/10.1016/j.envpol.2020.115465>.
- Kumar, Y., Mina, U., Rajput, V.D., Minkina, T., Kumar, S.N., Harit, R.C., Garg, M.C., 2023. Investigating the biochemical responses in wheat cultivars exposed to thermal power plant emission. *Bull. Environ. Contam. Toxicol.* 110, 1–8. <https://doi.org/10.1007/s00128-023-03719-3>.
- Latwal, M., Sharma, S., Kaur, I., Nagpal, A.K., 2023. Global assessment of air pollution indices of trees and shrubs for biomonitoring and green belt development – a tabulated review. *Water Air Soil Pollut.* 234, 205. <https://doi.org/10.1007/s11270-023-06194-y>.
- Lawlor, D.W., 2002. Limitation to photosynthesis in water-stressed leaves: stomata vs. metabolism and the role of ATP. *Ann. Bot.* 89, 871–885. <https://doi.org/10.1093/aob/mcf110>.
- Lehndorff, E., Schwark, L., 2004. Biomonitoring of air quality in the Cologne Combustion using pine needles as a passive sampler — Part II: polycyclic aromatic hydrocarbons (PAH). *Atmos. Environ.* 38, 3793–3808. <https://doi.org/10.1016/j.atmosenv.2004.03.065>.
- Leonard, R.J., McArthur, C., Hochuli, D.F., 2016. Particulate matter deposition on roadside plants and the importance of leaf trait combinations. *Urban For. Urban Green.* 20, 249–253. <https://doi.org/10.1016/j.ufug.2016.09.008>.
- Li, G.L., Lang, Y.H., Gao, M.S., Yang, W., Peng, P., Wang, X.M., 2014. Carcinogenic and mutagenic potencies for different PAHs sources in coastal sediments of Shandong Peninsula. *Mar. Pollut. Bull.* 84, 418–423. <https://doi.org/10.1016/j.marpolbul.2014.04.039>.
- Liu, X., Bai, Z., Yu, Q., Cao, Y., Zhou, W., 2017. Polycyclic aromatic hydrocarbons in the soil profiles (0–100 cm) from the industrial district of a large open-pit coal mine, China. *RSC Adv.* 7, 28029–28037. <https://doi.org/10.1039/C7RA02484C>.
- Liu, X., Shi, X.Q., Peng, Z.R., He, H.D., 2023. Quantifying the effects of urban fabric and vegetation combination pattern to mitigate particle pollution in near-road areas using machine learning. *Sustain. Cities Soc.* 93, 104524. <https://doi.org/10.1016/j.scs.2023.104524>.
- Li, X.B., Lu, Q.C., Lu, S.J., He, H.D., Peng, Z.R., Gao, Y., Wang, Z.Y., 2016. The impacts of roadside vegetation barriers on the dispersion of gaseous traffic pollution in urban street canyons. *Urban For. Urban Green.* 17, 80–91. <https://doi.org/10.1016/j.ufug.2016.03.006>.
- Li, X., Zhang, T., Sun, F., Song, X., Zhang, Y., Huang, F., Yuan, C., Yu, H., Zhang, G., Qi, F., Shao, F., 2021. The relationship between particulate matter retention capacity and leaf surface micromorphology of ten tree species in Hangzhou, China. *Sci. Total Environ.* 771, 144812. <https://doi.org/10.1016/j.scitotenv.2020.144812>.
- Li, Y., He, N., Hou, J., Xu, L., Liu, C., Zhang, J., Wang, Q., Zhang, X., Wu, X., 2018. Factors influencing leaf chlorophyll content in natural forests at the biome scale. *Front. Ecol. Evol.* 6, 1–10. <https://doi.org/10.3389/fevo.2018.00064>.
- Li, Y., Hoi, K.I., Mok, K.M., Yuen, K.V., 2023. Emerging air quality monitoring methods. In: Li, Y., Hoi, K.I., Mok, K.M., Yuen, K.V. (Eds.), *Air Quality Monitoring and Advanced Bayesian Modeling*. Elsevier, pp. 105–172. <https://doi.org/10.1016/B978-0-323-90266-3.00005-4>.
- Loppi, S., Pozo, K., Estellano, V.H., Corsolini, S., Sardella, G., Paoli, L., 2015. Accumulation of polycyclic aromatic hydrocarbons by lichen transplants: comparison with gas-phase passive air samplers. *Chemosphere* 134, 39–43. <https://doi.org/10.1016/j.chemosphere.2015.03.066>.
- Lukowski, A., Popek, R., Karolewski, P., 2020. Particulate matter on foliage of *Betula pendula*, *Quercus robur*, and *Tilia cordata*: deposition and ecophysiology. *Environ. Sci. Pollut. Res.* 27, 10296–11030. <https://doi.org/10.1007/s11356-020-07672-0>.
- Lu, T., Lin, X., Chen, J., Huang, D., Li, M., 2019. Atmospheric particle retention capacity and photosynthetic responses of three common greening plant species under different pollution levels in Hangzhou. *Glob. Ecol. Conserv.* 20, e00783. <https://doi.org/10.1016/j.gecco.2019.e00783>.
- Malav, L.C., Kumar, S., Islam, S., Chaudhary, P., Khan, S.A., 2022. Assessing the environmental impact of air pollution on crops by monitoring air pollution tolerance index (API) and anticipated performance index (API). *Environ. Sci. Pollut. Res.* 29, 50427–50442. <https://doi.org/10.1007/s11356-022-19505-3>.
- Mandal, K., Dhal, N.K., 2022. Pollution resistance assessment of plants around chromite mine based on anticipated performance index, dust capturing capacity and metal accumulation index. *Environ. Sci. Pollut. Res.* 29, 63357–63368. <https://doi.org/10.1007/s11356-022-20246-6>.
- Ma, Y., Wang, B., Zhang, R., Gao, Y., Zhang, X., Li, Y., Zuo, Z., 2019. Initial simulated acid rain impacts reactive oxygen species metabolism and photosynthetic abilities in *Cinnamomum camphora* undergoing high temperature. *Ind. Crop. Prod.* 135, 352–361. <https://doi.org/10.1016/j.indcrop.2019.04.050>.
- Morakinyo, O.M., Mukhola, M.S., Mokgobu, M.I., 2020. Concentration levels and carcinogenic and mutagenic risks of PM_{2.5}-bound polycyclic aromatic hydrocarbons in an urban-industrial area in South Africa. *Environ. Geochem. Health* 42, 2163–2178. <https://doi.org/10.1007/s10653-019-00493-2>.
- Mukherjee, A., Agrawal, S.B., Agrawal, M., 2020. Responses of tropical tree species to urban air pollutants: ROS/RNS formation and scavenging. *Sci. Total Environ.* 710, 1–14. <https://doi.org/10.1016/j.scitotenv.2019.136363>.

- Mukhopadhyay, S., Dutta, R., Dhara, A., Das, P., 2023. Biomonitoring of polycyclic aromatic hydrocarbons (PAHs) by *Murraya paniculata* (L.) Jack in South Kolkata, West Bengal, India: spatial and temporal variations. Environ. Geochem. Health 45, 5761–5781. <https://doi.org/10.1007/s10653-023-01506-x>.
- Nadgorska-Socha, A., Kandziora-Ciupa, M., Trzesicki, M., Barczyk, G., 2017. Air pollution tolerance index and heavy metal bioaccumulation in selected plant species from urban biotopes. Chemosphere 183, 471–482. <https://doi.org/10.1016/j.chemosphere.2017.05.128>.
- NAMP, 2023. National air quality monitoring program. URL: [https://cpcb.nic.in/abutnamp/](https://cpcb.nic.in/aboutnamp/).
- Nanos, G.D., Ilias, I.F., 2007. Effects of inert dust on olive (*Olea europaea* L.) leaf physiological parameters. Environ. Sci. Pollut. Res. 14, 212–214. <https://doi.org/10.1065/espr2006.08.327>.
- Ncube, B., Finnie, J.F., Van Staden, J., 2013. Dissecting the stress metabolic alterations in *in vitro Cyrtanthus* regenerants. Plant Physiol. Biochem. 65, 102–110. <https://doi.org/10.1016/j.phophys.2013.01.001>.
- Nisbet, I.C.T., Lagoy, P.K., 1992. Toxic equivalency factors (TEFs) for polycyclic aromatic hydrocarbons (PAHs). Regul. Toxicol. Pharmacol. 16, 290–300. [https://doi.org/10.1016/0273-2300\(92\)90009-X](https://doi.org/10.1016/0273-2300(92)90009-X).
- Niu, X., Wang, B., Wei, W., 2020. Response of the particulate matter capture ability to leaf age and pollution intensity. Environ. Sci. Pollut. Res. 27, 34258–34269. <https://doi.org/10.1007/s11356-020-09603-5>.
- Nizzetto, L., Pastore, C., Liu, X., Camporini, P., Stroppiana, D., Herbert, B., Boschetti, M., Zhang, G., Brivio, P.A., Jones, K.C., Di Guardo, A., 2008. Accumulation parameters and seasonal trend for PCBs in temperate and boreal forest plant species. Environ. Sci. Technol. 42, 5911–5916. <https://doi.org/10.1021/es800217m>.
- Ogunkunle, C.O., Suleiman, L.B., Oyedele, S., Awotoyer, O.O., Fatoba, P.O., 2015. Assessing the air pollution tolerance index and anticipated performance index of some tree species for biomonitoring environmental health. Agrofor. Syst. 89, 447–454. <https://doi.org/10.1007/s10457-014-9781-7>.
- Orecchio, S., 2010. Assessment of polycyclic aromatic hydrocarbons (PAHs) in soil of a Natural Reserve (Isola delle Femmine) (Italy) located in front of a plant for the production of cement. J. Hazard Mater. 173, 358–368. <https://doi.org/10.1016/j.jhazmat.2009.08.088>.
- Pandey, A.K., Pandey, M., Tripathi, B.D., 2015a. Air pollution tolerance index of climber plant species to develop vertical greenery systems in a polluted tropical city. Landsc. Urban Plann. 144, 119–127. <https://doi.org/10.1016/j.landurbplan.2015.08.014>.
- Pandey, A.K., Pandey, M., Mishra, A., Tiwary, S.M., Tripathi, B.D., 2015b. Air pollution tolerance index and anticipated performance index of some plant species for development of urban forest. Urban For. Urban Green. 14, 866–871. <https://doi.org/10.1016/j.ufug.2015.08.001>.
- Patel, K., Chaurasia, M., Rao, K.S., 2023. Urban dust pollution tolerance indices of selected plant species for development of urban greenery in Delhi. Environ. Monit. Assess. 195, 1–21. <https://doi.org/10.1007/s10661-022-10608-5>.
- Pathak, J., Rajneesh, Ahmed H., Singh, D.K., Singh, P.R., Kumar, D., et al., 2019. Oxidative stress and antioxidant defense in plants exposed to ultraviolet radiation. In: Hasanuzzaman, M., Fotopoulos, V., Nahar, K., Fujita, M. (Eds.), Reactive Oxygen, Nitrogen and Sulfur Species in Plants: Production, Metabolism, Signaling and Defense Mechanisms. John Wiley & Sons, Inc., pp. 371–420. <https://doi.org/10.1002/9781119468677.ch16>
- Pathak, V., Tripathi, B., Mishra, V., 2011. Evaluation of Anticipated Performance Index of some tree species for green belt development to mitigate traffic generated noise. Urban For. Urban Green. 10, 61–66. <https://doi.org/10.1016/j.ufug.2010.06.008>.
- Paull, N.J., Krix, D., Irga, P.J., Torpy, F.R., 2021. Green wall plant tolerance to ambient urban air pollution. Urban For. Urban Green. 63, 127201 <https://doi.org/10.1016/j.ufug.2021.127201>.
- Pereira, G.M., da Silva Caumo, S.E., do Nascimento, E.Q.M., Parra, Y.J., de Castro Vasconcellos, P., 2019. Polycyclic aromatic hydrocarbons in tree barks, gaseous and particulate phase samples collected near an industrial complex in São Paulo (Brazil). Chemosphere 237, 124499. <https://doi.org/10.1016/j.chemosphere.2019.124499>.
- Pereira, L.B.S., Costa-Silva, R., Felix, L.P., Agra, M.F., 2018. Leaf morphoanatomy of "mororo" (*Bauhinia* and *Schnella*, Fabaceae). Rev. Bras. Farmacogn. 28, 383–392. <https://doi.org/10.1016/j.bjph.2018.04.012>.
- Pleijel, H., Klingberg, J., Strandberg, B., Sjoman, H., Tarvainen, L., Wallin, G., 2022. Differences in accumulation of polycyclic aromatic compounds (PACs) among eleven broadleaved and conifer tree species. Ecol. Indicat. 145, 109681 <https://doi.org/10.1016/j.ecolind.2022.109681>.
- Popek, R., Gawronska, H., Gawronski, S.W., 2015. The level of particulate matter on foliage depends on the distance from the source of emission. Int. J. Phytoremediation 17, 1262–1268. <https://doi.org/10.1080/15226514.2014.989312>.
- Popek, R., Gawronska, H., Wrochna, M., Gawronski, S.W., Saebo, A., 2013. Particulate matter on foliage of 13 woody species: deposition on surfaces and phytostabilisation in waxes—a 3-year study. Int. J. Phytoremediation 15, 245–256. <https://doi.org/10.1080/15226514.2012.694498>.
- Popek, R., Mahawar, L., Shekhawat, G.S., Przybysz, A., 2022. Phyto-cleaning of particulate matter from polluted air by woody plant species in the near-desert city of Jodhpur (India) and the role of heme oxygenase in their response to PM stress conditions. Environ. Sci. Pollut. Res. 29, 70228–70241. <https://doi.org/10.1007/s11356-022-20769-y>.
- Porra, R.J., Scheer, H., 2019. Towards a more accurate future for chlorophyll a and b determinations: the inaccuracies of Daniel Arnon's assay. Photosynth. Res. 140, 215–219. <https://doi.org/10.1007/s11120-018-0579-8>.
- Pragasan, L.A., Ganesan, A., 2022. Assessment of air pollutants and pollution tolerant tree species for the development of Greenbelt at Narasapura Industrial Estate, India. Geol. Ecol. Landsc. <https://doi.org/10.1080/24749508.2022.2144857>.
- Prajapati, S.K., Tripathi, B.D., 2008a. Seasonal variation of leaf dust accumulation and pigment content in plant species exposed to urban particulates pollution. J. Environ. Qual. 37, 865–870. <https://doi.org/10.2134/jeq2006.0511>.
- Prajapati, S.K., Tripathi, B.D., 2008b. Anticipated Performance Index of some tree species considered for green belt development in and around an urban area: a case study of Varanasi city, India. J. Environ. Manag. 88, 1343–1349. <https://doi.org/10.1016/j.jenvman.2007.07.002>.
- Prusty, B.A.K., Mishra, P.C., Azeez, P.A., 2005. Dust accumulation and leaf pigment content in vegetation near the national highway at Sambalpur, Orissa, India. Ecotoxicol. Environ. Saf. 60, 228–235. <https://doi.org/10.1016/j.ecoenv.2003.12.013>.
- Przybysz, A., Nersisyan, G., Gawronski, S.W., 2019. Removal of particulate matter and trace elements from ambient air by urban greenery in the winter season. Environ. Sci. Pollut. Res. 26, 473–482. <https://doi.org/10.1007/s11356-018-3628-0>.
- Przybysz, A., Saebo, A., Hanslin, H.M., Gawronski, S.W., 2014. Accumulation of particulate matter and trace elements on vegetation as affected by pollution level, rainfall and the passage of time. Sci. Total Environ. 481, 360–369. <https://doi.org/10.1016/j.scitotenv.2014.02.072>.
- Pu, C., Xiong, J., Zhao, R., Fang, J., Liao, Y., Song, Q., Zhang, J., Zhang, Y., Liu, H., Liu, W., Chen, W., Zhou, H., Qi, S., 2022. Levels, sources, and risk assessment of polycyclic aromatic hydrocarbons (PAHs) in soils of karst trough zone, Central China. J. Hydrol. 614, 128568 <https://doi.org/10.1016/j.jhydrol.2022.128568>.
- Pugh, T.A.M., MacKenzie, A.R., Whyatt, J.D., Hewitt, C.N., 2012. Effectiveness of green infrastructure for improvement of air quality in urban street canyons. Environ. Sci. Technol. 46, 7692–7699. <https://doi.org/10.1021/es300826w>.
- Qazi, H.L., Jan, N., Ramazan, S., John, R., 2019. Protein modification in plants in response to abiotic stress. In: Dar, T.A., Singh, L.R. (Eds.), Protein Modificomics. Academic Press, pp. 171–201. <https://doi.org/10.1016/B978-0-12-811913-6.00008-4>.
- Qiu, Y., Guan, D., Song, W., Huang, K., 2009. Capture of heavy metals and sulfur by foliar dust in urban Huizhou, Guangdong Province, China. Chemosphere 75, 447–452. <https://doi.org/10.1016/j.chemosphere.2008.12.061>.
- Rai, P.K., 2016. Impacts of particulate matter pollution on plants: implications for environmental biomonitoring. Ecotoxicol. Environ. Saf. 129, 120–136. <https://doi.org/10.1016/j.ecoenv.2016.03.012>.
- Rangani, J., Panda, A., Patel, M., Parida, A.K., 2018. Regulation of ROS through proficient modulations of antioxidative defense system maintains the structural and functional integrity of photosynthetic apparatus and confers drought tolerance in the facultative halophyte *Salvadora persica* L. J. Photochem. Photobiol. B 189, 214–233. <https://doi.org/10.1016/j.jphotobiol.2018.10.021>.
- Raza, A., Charagh, S., Abbas, S., Hassan, M.U., Saeed, F., Haider, S., Sharif, R., Anand, A., Corpas, F.J., Jin, W., Varshney, R.K., 2023. Assessment of proline function in higher plants under extreme temperatures. Plant Biol. 25, 379–395. <https://doi.org/10.1111/plb.13510>.
- Redondo-Bermudez, M.D.C., Gulenc, I.T., Cameron, R.W., Inkson, B.J., 2021. 'Green barriers' for air pollutant capture: leaf micromorphology as a mechanism to explain plants capacity to capture particulate matter. Environ. Pollut. 288, 117809 <https://doi.org/10.1016/j.envpol.2021.117809>.
- Roy, A., Bhattacharya, T., Kumari, M., 2020. Air pollution tolerance, metal accumulation and dust capturing capacity of common tropical trees in commercial and industrial sites. Sci. Total Environ. 722, 137622 <https://doi.org/10.1016/j.scitotenv.2020.137622>.
- Saebo, A., Popok, R., Nawrot, B., Hanslin, H.M., Gawronska, H., Gawronski, S.W., 2012. Plant species differences in particulate matter accumulation on leaf surfaces. Sci. Total Environ. 427–428, 347–354. <https://doi.org/10.1016/j.scitotenv.2012.03.084>.
- Sameena, P.P., Puthur, J.T., 2021. Differential modulation of photosynthesis and defense strategies towards copper toxicity in primary and cotyledonary leaves of *Ricinus communis* L. J. Photochem. Photobiol. A 8, 100059. <https://doi.org/10.1016/j.jpp.2021.100059>.
- Sarabi, V., Arjomand-Ghajur, E., 2021. Exogenous plant growth regulators/plant growth promoting bacteria roles in mitigating water-deficit stress on chicory (*Cichorium pumilum* Jacq.) at a physiological level. Agric. Water Manag. 245, 106439 <https://doi.org/10.1016/j.agwat.2020.106439>.
- Saxena, P., Kulshrestha, U., 2016. Biochemical effects of air pollutants on plants. In: Kulshrestha, U., Saxena, P. (Eds.), Plant Responses to Air Pollution. Springer, Singapore, pp. 59–70. https://doi.org/10.1007/978-981-10-1201-3_6.
- Seenu, Y., Ravichandran, K.R., Sivadas, A., Mayakrishnan, B., Thangavelu, M., 2019. Vegetative anatomy of *Tabernaemontana alternifolia* L. (Apocynaceae) endemic to southern Western Ghats, India. Acta Biol. Szeged. 63, 185–193. <http://abs.bibl.u-szeged.hu/index.php/abs>.
- Shabala, S., Cuin, T.A., 2008. Potassium transport and plant salt tolerance. Physiol. Plantarum 133, 651–669. <https://doi.org/10.1111/j.1399-3054.2007.01008.x>.
- Shabnam, N., Oh, J., Park, S., Kim, H., 2021. Impact of particulate matter on primary leaves of *Vigna radiata* (L.) Wilczek. Ecotoxicol. Environ. Saf. 212, 111965 <https://doi.org/10.1016/j.ecoenv.2021.111965>.
- Shabnam, N., Sharmila, P., Sharma, A., Strasser, R.J., Pardha-Saradhi, P., 2015. Mitochondrial electron transport protects floating leaves of long leaf pondweed (*Potamogeton nodosus* Poir) against photoinhibition: comparison with submerged leaves. Photosynth. Res. 125, 305–319. <https://doi.org/10.1007/s11120-014-0051-3>.
- Shah, K., An, N., Ma, W., Ara, G., Ali, K., Kamanova, S., Zuo, X., Han, M., Ren, X., Xing, L., 2020. Chronic cement dust load induce novel damages in foliage and buds of *Malus domestica*. Sci. Rep. 10, 1–12. <https://doi.org/10.1038/s41598-020-68902-6>.

- Shanazari, M., Golkar, P., Mirmohammady Maibody, A.M., 2018. Effects of drought stress on some agronomic and bio-physiological traits of *Triticum aestivum*, *Triticale*, and *Tritipyrum* genotypes. *Arch. Agron. Soil Sci.* 64, 2005–2018. <https://doi.org/10.1080/03650340.2018.1472377>.
- Shao, F., Wang, L., Sun, F., Li, G., Yu, L., Wang, Y., Zeng, X., Yan, H., Dong, L., Bao, Z., 2019. Study on different particulate matter retention capacities of the leaf surfaces of eight common garden plants in Hangzhou, China. *Sci. Total Environ.* 652, 939–951. <https://doi.org/10.1016/j.scitotenv.2018.10.182>.
- Sharma, A.P., Tripathi, B.D., 2009. Assessment of atmospheric PAHs profile through *Calotropis gigantea* R.Br. leaves in the vicinity of an Indian coal-fired power plant. *Environ. Monit. Assess.* 149, 477–482. <https://doi.org/10.1007/s10661-008-0224-7>.
- Sharma, B., Bhardwaj, S.K., Sharma, S., Nautiyal, R., Kaur, L., Alam, N.M., 2019. Pollution tolerance assessment of temperate woody vegetation growing along the National Highway-5 in Himachal Pradesh, India. *Environ. Monit. Assess.* 191, 1–14. <https://doi.org/10.1007/s10661-019-7310-x>.
- Shrivastava, R., Mishra, A., 2018. Air pollution induced changes in foliar micro-morphology of roadside shrub species, *Thevetia peruviana* and *Plumeria alba* in Rewa City, MP, India. *Int. Res. J. Environ. Sci.* 7, 1–7.
- Shukla, S., Khan, R., Bhattacharya, P., Devanesan, S., AlSalhi, M.S., 2022. Concentration, source apportionment and potential carcinogenic risks of polycyclic aromatic hydrocarbons (PAHs) in roadside soils. *Chemosphere* 292, 133413. <https://doi.org/10.1016/j.chemosphere.2021.133413>.
- Singh, A.K., Kumar, M., Bauddh, K., Singh, A., Singh, P., Madhav, S., Shukla, S.K., 2023. Environmental impacts of air pollution and its abatement by plant species: a comprehensive review. *Environ. Sci. Pollut. Res.* 30, 79587–79616. <https://doi.org/10.1007/s11356-023-28164-x>.
- Singh, H.P., Batish, D.R., Kohli, R.K., Arora, K., 2007. Arsenic-induced root growth inhibition in mung bean (*Phaseolus aureus* Roxb.) is due to oxidative stress resulting from enhanced lipid peroxidation. *Plant Growth Regul.* 53, 65–73. <https://doi.org/10.1007/s10725-007-9205-z>.
- Singh, S., Gupta, N.C., Bhattacharya, P., 2016. Morphological study of leaf epidermis for *Alstonia scholaris* (L.) R. Br at institutional site of urban Delhi. In: Kumar, S., Beg, M. A., Sayeed, M.T. (Eds.), *Environmental Concerns of 21st Century: Indian and Global Context*. Book Age Publications, Delhi, India, pp. 235–246.
- Singh, S.K., Rao, D.N., Agrawal, M., Pandey, J., Naryan, D., 1991. Air pollution tolerance index of plants. *J. Environ. Manag.* 32, 45–55. [https://doi.org/10.1016/S0301-4797\(05\)80080-5](https://doi.org/10.1016/S0301-4797(05)80080-5).
- Stefi, A.L., Mitsigiorgi, K., Vassilacopoulou, D., Christodoulakis, N.S., 2020. Response of young *Nerium oleander* plants to long-term non-ionizing radiation. *Planta* 251, 1–17. <https://doi.org/10.1007/s00425-020-03405-2>.
- Sudhakar, P., Latha, P., Reddy, P.V., 2016. Phenotyping Crop Plants for Physiological and Biochemical Traits. Academic Press, p. 194. <https://doi.org/10.1016/C2015-0-01450-2>.
- Terzaghi, E., Zaccarello, G., Scacchi, M., Raspa, G., Jones, K.C., Cerabolini, B., Guardo, A. D., 2015. Towards more ecologically realistic scenarios of plant uptake modelling for chemicals: PAHs in a small forest. *Sci. Total Environ.* 505, 329–337. <https://doi.org/10.1016/j.scitotenv.2014.09.108>.
- Thompson, J.E., 2018. Airborne particulate matter: human exposure & health effects. *J. Occup. Environ. Med.* 60, 392–423.
- Thunis, P., Clappier, A., Tarrason, L., Cuvelier, C., Monteiro, A., Pisoni, E., Wesseling, J., Belis, C.A., Pirovano, G., Janssen, S., Guerreiro, C., Peduzzi, E., 2019. Source apportionment to support air quality planning: Strengths and weaknesses of existing approaches. *Environ. Int.* 130, 104825. <https://doi.org/10.1016/j.envint.2019.05.019>.
- Tian, L., Yin, S., Ma, Y., Kang, H., Zhang, X., Tan, H., Meng, H., Liu, C., 2019. Impact factor assessment of the uptake and accumulation of polycyclic aromatic hydrocarbons by plant leaves: morphological characteristics have the greatest impact. *Sci. Total Environ.* 652, 1149–1155. <https://doi.org/10.1016/j.scitotenv.2018.10.357>.
- Tong, S.T.Y., 1991. The retention of copper and lead particulate matter in plant foliage and forest soil. *Environ. Int.* 17, 31–37. [https://doi.org/10.1016/0160-4120\(91\)90335-N](https://doi.org/10.1016/0160-4120(91)90335-N).
- USEPA, 2002. Peer Consultation Workshop on Approaches to Polycyclic Aromatic Hydrocarbon (PAH) Health Assessment. U.S. Environmental Protection Agency, Office of Research and Development, National Center for Environmental Assessment, Washington Office, Washington, DC. EPA/635/R-02/005. <https://cfpub.epa.gov/necearisk/recordisplay.cfm?deid=54787>.
- Venkatesan, P., 2016. WHO report: air pollution is a major threat to health. *Lancet Respir. Med.* 4, 351. [https://doi.org/10.1016/S2213-2600\(16\)30014-5](https://doi.org/10.1016/S2213-2600(16)30014-5).
- Verma, P.K., Sah, D., Satish, R., Rastogi, N., Kumari, K.M., Lakhani, A., 2022. Atmospheric chemistry and cancer risk assessment of polycyclic aromatic hydrocarbons (PAHs) and nitro-PAHs over a semi-arid site in the Indo-Gangetic plain. *J. Environ. Manag.* 317, 115456. <https://doi.org/10.1016/j.jenvman.2022.115456>.
- Wang, J., Bao, H., Zhang, H., Li, J., Hong, H., Wu, F., 2020. Effects of cuticular wax content and specific leaf area on accumulation and partition of PAHs in different tissues of wheat leaf. *Environ. Sci. Pollut. Res.* 27, 18793–18802. <https://doi.org/10.1007/s11356-020-08409-z>.
- Weerakkody, U., Dover, J.W., Mitchell, P., Reiling, K., 2018. Evaluating the impact of individual leaf traits on atmospheric particulate matter accumulation using natural and synthetic leaves. *Urban For. Urban Green.* 30, 98–107. <https://doi.org/10.1016/j.ufug.2018.01.001>.
- WHO, 2000. *Air Quality Guidelines for Europe. European Series No 91*, World Health Organization, WHO Regional Publications, Geneva.
- WHO, 2006. Regional Office for Europe & Joint WHO/Convention Task force on the health aspects of air pollution. *Health Risks of Particulate Matter from Long-Range Transboundary Air Pollution*. WHO Regional Office for Europe, Copenhagen, p. 99. <https://apps.who.int/iris/handle/10665/107691>.
- Wu, J., Luo, K., Wang, Y., Wang, Z., 2021. Urban road greenbelt configuration: the perspective of PM_{2.5} removal and air quality regulation. *Environ. Int.* 157, 106786. <https://doi.org/10.1016/j.envint.2021.106786>.
- Xia, J., Yuan, W., Wang, Y.P., Zhang, Q., 2017. Adaptive carbon allocation by plants enhances the terrestrial carbon sink. *Sci. Rep.* 7, 1–11. <https://doi.org/10.1038/s41598-017-03574-3>.
- Xie, C., Guo, J., Yan, L., Jiang, R., Liang, A., 2022. The influence of plant morphological structure characteristics on PM_{2.5} retention of leaves under different wind speeds. *Urban For. Urban Green.* 71, 127556. <https://doi.org/10.1016/j.ufug.2022.127556>.
- Xu, H., Wang, W., Wang, H., Sun, Y., Zhong, Z., Wang, S., 2019. Differences in quantity and composition of leaf particulate matter and morphological structures in three evergreen trees and their association in Harbin, China. *Environ. Pollut.* 252, 1772–1790. <https://doi.org/10.1016/j.envpol.2019.06.124>.
- Yaghmaei, L., Jafari, R., Soltani, S., Eshghizadeh, H.R., Jahanbazy, H., 2022. Interaction effects of dust and water deficit stresses on growth and physiology of Persian oak (*Quercus brantii* Lindl.). *J. Sustain. For.* 41, 134–158. <https://doi.org/10.1080/10549811.2020.1845742>.
- Yang, B., Liu, S., Liu, Y., Li, X., Lin, X., Liu, M., Liu, X., 2017. PAHs uptake and translocation in *Cinnamomum camphora* leaves from Shanghai, China. *Sci. Total Environ.* 574, 358–368. <https://doi.org/10.1016/j.scitotenv.2016.09.058>.
- Zhang, P.Q., Liu, Y.J., Chen, X., Yang, Z., Zhu, M.H., Li, Y.P., 2016. Pollution resistance assessment of existing landscape plants on Beijing streets based on air pollution tolerance index method. *Ecotoxicol. Environ. Saf.* 132, 212–223. <https://doi.org/10.1016/j.ecoenv.2016.06.003>.
- Zhang, W., Zhang, Y., Gong, J., Yang, B., Zhang, Z., Wang, B., Zhu, C., Shi, J., Yue, K., 2020. Comparison of the suitability of plant species for greenbelt construction based on particulate matter capture capacity, air pollution tolerance index, and antioxidant system. *Environ. Pollut.* 263, 114615. <https://doi.org/10.1016/j.envpol.2020.114615>.
- Zhang, X., Wang, J., Feng, S., Yu, X., Zhou, A., 2022. Morphological and physiological responses of *Dianthus caryophyllus* high wax mutant to low-temperature stress. *J. Plant Physiol.* 275, 153762. <https://doi.org/10.1016/j.jplph.2022.153762>.
- Zhou, Y., Chen, C., Lu, T., Zhang, J., Chen, J., 2022. Season impacts on estimating plant's particulate retention: field experiments and meta-analysis. *Chemosphere* 288, 132570. <https://doi.org/10.1016/j.chemosphere.2021.132570>.
- Zilaie, M.N., Arani, A.M., Etesami, H., 2023. Evaluation of air pollution (dust) tolerance index of three desert species *Seidlitzia rosmarinus*, *Haloxylon aphyllum*, and *Nitraria schoberi* under salinity stress. *Environ. Monit. Assess.* 195, 1–13. <https://doi.org/10.1007/s10661-023-11436-x>.